NASA TN D-195



# TECHNICAL NOTE

## D-195

# EVOLUTION OF AMPLIFIED WAVES LEADING TO TRANSITION IN A BOUNDARY LAYER WITH ZERO PRESSURE GRADIENT

By P. S. Klebanoff and K. D. Tidstrom
National Bureau of Standards

NATIONAL AERONAUTICS AND SPACE ADMINISTRATION
WASHINGTON
September 1959

NATIONAL AERONAUTICS AND SPACE ADMINISTRATION

TECHNICAL NOTE D-195

# EVOLUTION OF AMPLIFIED WAVES LEADING TO TRANSITION IN A BOUNDARY LAYER WITH ZERO PRESSURE GRADIENT

By P. S. Klebanoff and K. D. Tidstrom



## SUMMARY

The results of an experimental investigation of the instability of a laminar boundary layer leading to transition are presented. Waves were introduced into the boundary layer of a flat plate using the vibrating-ribbon technique, and their development and subsequent breakdown were studied using the hot-wire anemometer as the principal measuring device. Certain significant features of the wave behavior have been revealed. The motions leading to transition are strongly three-dimensional, and the nature of this three-dimensionality has been investigated. The effect of the wave on the mean flow and its behavior in relation to the Tollmien-Schlichting theory were also studied. It is demonstrated that associated with the wave growth there is present an energy-concentrating mechanism involving the transfer of wave energy from one spanwise position to another resulting in streetlike concentrations of wave energy. It is also shown that the initial breakdown of laminar flow is of small extent and may be loosely described as pointlike. Breakdown of the laminar flow occurs in the outer region of the layer, and intermittent separation was not involved in the transition process described herein.

## INTRODUCTION

In the last decade there has been renewed emphasis on the boundary-layer transition problem. Although the stability theories provided information on the behavior of perturbations and the critical Reynolds number for which a laminar boundary layer is unstable, the inherent limitations of the theories arising from their linear character render them powerless to describe the actual breakdown of laminar flow. Thus, at the present time, one must depend on experiment to bridge the gap between the wave motion associated with the unstable laminar boundary layer and the actual occurrence of transition. Much of the recent work has been done at supersonic speeds, where so far the emphasis has been

placed mainly on effects of various flow and thermal conditions on transition Reynolds numbers. Because of the many factors influencing transition, the results have been difficult to interpret, and only indirect hints concerning a mechanism of transition are obtainable. A notable exception has been the work of Laufer and Vrebalovich (ref. 1) where use was made of the hot-wire technique to detect the presence of Tollmien-Schlichting-like waves in the supersonic boundary layer. This strengthens the point of view that the underlying mechanism of transition is essentially the same at both subsonic and supersonic speeds.

Several years ago the National Bureau of Standards undertook an extensive experimental investigation of boundary-layer transition at subsonic speeds (less than 100 ft/sec). In this speed range the hot-wire anemometer can be used to good advantage. The aim has been to investigate the mechanics of transition, that is, how the laminar flow breaks down into turbulent flow, and how the turbulent boundary layer comes into being. In a previous report (ref. 2) the nature of the transition region is clearly defined. This work confirms the spot theory of turbulence as postulated by Emmons (ref. 3). It was shown that transition is a process which develops as the flow progresses downstream, beginning with growing perturbations that then produce turbulent spots which in turn grow as they move on downstream to consume intervening laminar regions. Rate of propagation, shape, and other significant features of the turbulent spot were studied. The difficulty in finding the location of the initial breakdown of laminar flow, and the existence of transverse as well as streamwise spot growth implied that the original breakdown was pointlike. In order to further investigate this question, as well as others pertaining to three-dimensional effects, intermittent separation, and the behavior of finite amplitude waves, the present phase of the investigation was undertaken. It is also shown in reference 2 that there is a direct dependence of transition on Tollmien-Schlichting waves in the boundary layer, and it was felt that the best procedure would be to observe by hot-wire techniques the growth and evolution of a wave from its source to transition under controlled conditions. It was possible to carry out this objective by using the vibrating-ribbon technique used by Schubauer and Skramstad (ref. 4) in their experimental confirmation of the Tollmien-Schlichting stability theory (refs. 5 to 7).

The investigation was conducted under the sponsorship and with the financial assistance of the National Advisory Committee for Aeronautics.

A shortened account of the investigation was presented by Schubauer at the Symposium on Boundary Layer Research held in Freiburg, Germany, in August of 1957 (ref. 8). The authors wish to express their appreciation for the active interest, encouragement, and advice of Dr. Schubauer and to gratefully acknowledge the assistance of Mr. Lee Sargent in the experimental program.

## SYMBOLS

| | |
|---|---|
| $f$ | wave frequency |
| $p$ | static pressure |
| $p_o$ | static pressure at $x = 10.5$ feet |
| $q_o$ | free-stream dynamic pressure |
| $Re_{\delta^*}$ | Reynolds number based on boundary-layer displacement thickness, $\left(\frac{U_1 \delta^*}{\nu}\right)$ |
| $r$ | streamline radius of curvature |
| $t$ | time |
| $U$ | local mean velocity in boundary layer |
| $U_1$ | mean velocity in free stream |
| $u,v,w$ | instantaneous velocity fluctuations in x-, y-, and z-directions, respectively |
| $u',v',w'$ | root-mean-square values of $u$, $v$, and $w$ |
| $u'_o$ | root-mean-square value of $u$ at $x_o$ |
| $\overline{uv},\overline{uw}$ | Reynolds stresses |
| $\overline{wu^2}$ | spanwise energy transfer rate |
| $x$ | distance along surface from leading edge of flat plate |
| $x_o$ | reference position 2 in. downstream from ribbon |
| $x_1$ | distance downstream from vibrating ribbon |
| $y$ | distance normal to surface, measured from surface |
| $\Delta y$ | streamline displacement |
| $z$ | spanwise direction perpendicular to x,y-plane |
| $\beta_r$ | $2\pi f$ |

| | |
|---|---|
| $\delta$ | boundary-layer thickness |
| $\delta^*$ | boundary-layer displacement thickness |
| $\lambda$ | wave length |
| $\nu$ | kinematic viscosity |
| $\rho$ | density |
| $\Phi$ | phase angle between u- and w-fluctuations |



## EXPERIMENTAL ARRANGEMENT AND PROCEDURE

### Wind Tunnel and Flat Plate

The investigation was conducted at the Bureau of Standards in the $4\frac{1}{2}$-foot wind tunnel on an aluminum flat plate, $4\frac{1}{2}$ feet wide, 12 feet long, and 1/4 inch thick with a symmetrically tapered and sharpened leading edge. The plate was mounted vertically in the center of the test section. A positive angle of attack was obtained by displacing the leading edge and by the use of additional blocking at the downstream end of the working side of the plate. This was done in order to shift the stagnation point to the working side of the plate and to have smooth flow conditions at the leading edge. A false wall made of sheet aluminum was mounted on the tunnel wall opposite the working side of the plate and was adjusted to give zero pressure gradient along the surface. The pressure gradient is shown in figure 1. The small variations in the pressure gradient were associated with the inherent waviness of the surface and could not be removed by adjusting the false wall. All measurements were made at a free-stream speed of about 50 feet per second. The speed was changed within moderate limits to keep a constant Reynolds number per foot equal to $3.03 \times 10^5$. At this Reynolds number natural transition occurred about 8 feet from the leading edge. The turbulence level of the tunnel was 0.03 percent.

### Vibrating Ribbon

The method for exciting waves in the laminar boundary layer is the same as that described in reference 4. A thin brass ribbon, 3 feet long, 0.002 inch thick, and 3/32 inch wide was mounted in the boundary layer transverse to the flow 0.009 inch from the surface and 2.92 feet from the leading edge. This position corresponds to $Re_{\delta^*} = 1620$. The active section of the ribbon was reduced to a segment 13 inches long at the

midspan of the plate. Patches of scotch tape served as spacers and insulators. In the presence of a magnetic field from an electromagnet mounted on the opposite side of the plate, the segment was made to vibrate to and from the plate in a single loop by passing through the ribbon an alternating current of the desired frequency from a variable-frequency oscillator feeding into a power amplifier. The ribbon was kept under tension and the resonant frequency was kept near the working frequency by means of the rubber-band suspension at the extreme ends. Neither changes in the vibrating span nor in the spacing from the plate had any appreciable effect on the character of the wave generated.



## Traversing Mechanism

The traversing unit used for traversing in a spanwise direction as well as in a direction normal to the surface is shown in figure 2. By means of the brackets shown in the figure the unit was bolted to a streamlined strut so that the legs rested firmly against the surface. In this position the unit was used for spanwise traversing with a usable travel of 4 inches. By removing the legs and rotating the unit 90° to place the end opposite the gears against the surface, the movement was oriented for traversing normal to the surface. A micrometer screw of 0.5-millimeter pitch was driven through a set of beveled gears and a shaft by a pulley arrangement. The motor driving the pulley is not shown in the figure. It is a small 10-rpm a-c motor with a 2- by 2-inch housing which was mounted on the strut 10 inches below the traverse. There are ten prongs on the pulley, and the number of contacts these made with the microswitch was counted by an electronic counter to determine position. One of the two measuring probes was driven by the screw; the other could be manually moved relative to the other and was in general used to monitor the wave. The measuring probes were attached so that they could move fore and aft and rotate in a vertical plane to provide for ease of alinement. Manually operated screw adjustments were provided for each probe so that they could be positioned in a direction normal to that in which the traversing was done. The probes extended 9 inches upstream from the point of support to avoid interference effects. The alinement with respect to the plate was such that in a spanwise travel of 4 inches the probe did not ride off more than 0.002 inch. Initial distance from the surface was obtained by using a prism to reflect the probe and its image on the calibrated scale of a microscope.

When traversing at fixed y- and z-positions, but varying x-position, small sledlike arrangements resting under tension against the surface, and sometimes carrying two hot wires with fixed displacement in the y- or z-direction, were attached by means of a long arm (carrying hot-wire leads) to the strut. Channel irons attached to the floor and ceiling of the tunnel served as guide rails for the strut, which could be moved longitudinally by means of a chain and sprocket operated from outside the tunnel.

### Measurement of Mean Flow and Fluctuation Quantities

The impact and static-pressure probes used in the measurement of mean-velocity and pressure distribution were made of nickel tubing 0.04 inch in diameter and 0.003 inch in wall thickness. The static-pressure tube was made according to the conventional design for such a tube, and the pressure distribution was measured by traversing longitudinally at a distance 0.25 inch from the surface. The impact tube was flattened at the end to form a rectangular opening 0.01 inch wide and together with a static tube similar to that used for the pressure distribution was used to measure mean velocity. Mean velocities were also obtained during the course of hot-wire measurements of the fluctuations.

The fluctuation quantities measured were $u'$, $w'$, $\overline{uw}$, and $\overline{wu^2}$. The hot-wire equipment used is similar to that described in reference 9, and a description of the methods used in the measurement of these various quantities except for $\overline{wu^2}$ is given in reference 10. Platinum wires 0.0001 inch in diameter and about 1 millimeter long were used. Measurements involving the use of two wires were made using a V-wire arrangement rather than the customary X-type in order to avoid difficulty from the steep gradients across the boundary layer. As a result of the steep gradient no measurements of $v'$ have as yet been attempted. The separation between centers of the wires in the V-wire arrangement was 0.5 millimeter. In the measurement of $\overline{wu^2}$, the sum of the output of the two wires was used to give $u(t)$, which was squared by an instantaneous squaring circuit and then combined by the sum and difference method with the difference signal of the two wires $w(t)$ to obtain $\overline{wu^2}$. Measurements of $u'$ and $w'$ were obtained at the same time. A separate check on the $u'$ obtained from the V-wire arrangement with that obtained with the usual normal wire method agreed to within a few percent. In cases where $u'$ is compared with any of the other quantities, it was obtained with the V-wire arrangement. Film recording of the $u$ and $w$ fluctuation from a dual-beam cathode-ray oscilloscope was useful, and at times the signals from two hot wires sensitive to the u-fluctuation were also observed simultaneously.

## RESULTS AND DISCUSSION

### Three-Dimensional Nature of Wave

Figure 3 shows the spanwise distribution of intensity of the longitudinal fluctuation $u$ for a 145-cps wave measured at a fixed distance from the wall ($y = 0.046$ in.) for different positions downstream from the vibrating ribbon. This y-position was chosen because it is in the vicinity of the critical layer, and is about the position where the

distribution of amplitude of the wave across the boundary layer has its maximum for the Tollmien-Schlichting distribution. It is seen that there has developed a strong three-dimensionality, as shown by the large variation of intensity at peaks and valleys of the distribution. The peaks and valleys maintain a fixed spanwise position as they intensify in a downstream direction with breakdown of the wave occurring at a peak. There is no evidence of breakdown at the valley until the disturbance generated at the peak has spread to the valley. A typical breaking pattern associated with transition and accompanying the wave at $x_1 = 13$ inches is also shown. The oscillogram was obtained at $y = 0.12$ inch, which correspondes to about 0.6 $\delta$. This is in the region where the characteristic breakdown of the wave as shown is most intense and where the breakdown appears to originate. The breaking pattern at the peak consists of bursts of high-frequency fluctuations in the direction of lower velocities and occurs once each cycle of the basic wave. These bursts are evidently a streetlike succession of turbulent spots in an early stage of development. They are further discussed in the section Wave Breakdown. The initial breakdown of the wave for the condition shown in figure 3 occurred between $x_1 = 10$ inches and $x_1 = 13$ inches. After breakdown the measurements were more difficult, as evidenced by the scatter.

The variation in intensity had its beginning well upstream from transition, where the wave is still quite pure. A puzzling feature of the three-dimensionality was the fact that the spacing between peaks and valleys was invariant to changes in experimental conditions. It is not spurious in the sense that it is introduced by the vibrating ribbon. As far as could be detected by visual means, the ribbon vibrated in a single loop and had an essentially uniform amplitude for the middle 6 inches of its span. Varying the width, span, and distance from the surface of the vibrating ribbon, as well as moving it to different positions on the plate and changing the design of the electromagnet, all had no effect on the spatial variations observed. It was eventually established that there existed a direct connection between the spacing of peaks and valleys in figure 3 and the existence of spanwise mean-flow variations in the laminar layer. Figure 4 shows the spanwise distribution of mean velocity measured with a pitot-static arrangement at $x = 3.5$ feet for different positions across the boundary layer. These velocity differences were not caused by the waves. The open-circle symbols represent measurements obtained with the ribbon removed from the plate. The triangular symbols shown at $y = 0.098$ inch represent measurements obtained with the ribbon vibrating so that the wave intensity is of the magnitude shown in figure 3. Spanwise velocity differences as large as 10 percent existed. They existed only in the boundary layer and were not present in the free stream. Spanwise surveys of mean velocity were also made at 2 and 4 feet from the leading edge, and the same behavior as shown in figure 4 was observed. Apparently the spanwise variations of velocity

were in the boundary layer from its beginning, and like the peaks and valleys that accompany the wave intensity, their z-position remained fixed in the downstream direction. The striking fact is that, as shown in figure 5, peaks and valleys which accompany the wave coincide with the maximum and minimum of the mean velocity. Figure 6 shows the velocity distribution across the boundary layer at two representative z-positions corresponding to a maximum and minimum, compared with the Blasius distribution. The almost periodic variations are apparently due to weak longitudinal vortices which manifest themselves in a spanwise thickening and thinning of the layer with no noticeable effect on the velocity profile, which is still of the Blasius type. This affords a plausible explanation for the relation between the mean flow and wave shown in figure 5. The spanwise variation in boundary-layer thickness coupled with the circumstance that the 145-cps wave lies near branch II of the Tollmien-Schlichting stability diagram gives rise to local variations in amplification rate in such a direction that where the layer is thicker the amplification becomes less than where it is thinner. The same reasoning suggests that the converse should be true for a frequency near branch I of the stability diagram, and that by choosing a frequency near branch I the peaks and valleys of figure 4 should be reversed. This explanation is supported by the effect shown in figure 7, where the spanwise variations in wave intensity are compared for frequencies of 65, 80, and 145 cps. The amplitude of the ribbon for each frequency was adjusted to give about the same level of intensity at $z = 1.5$ inch, and measurements of intensity were made at the peak and valley positions of figure 3. The curves connecting the measured points are dashed, since no measurements were made in between. Comparison of the 145-cps wave, which lies near branch II, and the 65-cps wave, which lies near branch I, shows that their peaks and valleys are interchanged. The 80-cps wave, which is still on the branch I side of the stability diagram but close to its middle where the amplification rate is less sensitive to Reynolds number, exhibits less irregularity.

Leading-edge and surface conditions were found to play no role in establishing the mean-flow variations. The surface in addition to being cleaned and waxed was covered with a 1/16-inch-thick Formica sheet, to produce a new surface and a new leading edge, and no effect could be observed. The positive angle of attack which the plate made with the wind stream was also investigated because of the possibility proposed by Gortler that the concave curvature associated with the incident streamlines may generate longitudinal vortices. The angle of attack was decreased to the point where occasional bursts of turbulence due to leading-edge conditions set in and no difference was found. The only feature of the experimental environment which had any influence was the wind-tunnel damping screens located in the settling chamber at a considerable distance upstream from the plate. Cleaning the screens modified the variations by shifting their positions on the plate and altering

their magnitude but did not eliminate them. In all cases the spacing was of the order of 1 inch. When the spanwise position of the mean-velocity variations was changed, the peaks and valleys of the wave shifted accordingly, giving further evidence of their connection. In addition, the spacing of the peaks and valleys was markedly sensitive to the mean-velocity variations. Spanwise differences of only a few percent in the mean velocity were able to establish their spacing. By choosing a wave of proper frequency, that is, one which is not sensitive to the local variations in Reynolds number, the degree of irregularity initially present in the wave could be markedly reduced. However, if the amplitude of the wave was increased, peaks and valleys again developed, although the Reynolds number range remained the same. This indicates that the large variations in intensity shown in figure 3 are not solely a consequence of the local variations in their amplification rate, as given by linear theory, and that the role played by the mean velocity is not so much to determine the magnitude of the difference between peak and valley as it is to determine spacing and initial irregularity. Thus, it appears that the wave has an inherent tendency to develop peaks and valleys in amplitude which always develop before transition occurs. It is planned to investigate the experimental environment further by installing new damping screens. In addition to the intrinsic nature of the phenomenon, it is a realistic condition inasmuch as waves in natural transition arising from random disturbances are apt to be distorted. Also, the wave most amplified is naturally near branch II of the neutral curve and is especially susceptible to irregularities in the mean flow.

## Wave Growth and Effect on Mean Flow

Figures 8 and 9 show the growth in wave intensity from the ribbon to transition at a frequency of 145 cps for different input levels of the vibrating ribbon. The measurements were made along lines corresponding to a peak and a neighboring valley at a fixed distance $y = 0.046$ inch from the wall, and beginning at $x_0$, which is a reference position 2 inches downstream from the ribbon. The peak and valley positions were 0.4 inch apart in the z-direction. At the low-amplitude levels of curves A, an analyzer with an effective band width of 5.3 cycles was used to eliminate the background level. At the higher amplitudes of curves B, C, and D the background level was not troublesome. The low-amplitude waves for peak and valley (curves A), which amplify and then damp, are taken to be those characteristic of the linear theory. When subsequent mention is made of linear amplification rate, the term will mean amplification as governed by the linear theory, not a linear variation in the rate itself. The Tollmien-Schlichting theory has been well verified (ref. 4), and since the purpose of the present investigation is to study the region of finite amplitude, where the theory is no longer applicable, no direct comparison of amplification rates with those given by theory

is made. Consequently no attempt was made to refine the experimental procedure as required for a quantitative check of theory. However, the general features of the wave such as its neutral position and wave velocity agree quite well with theory. As is consistent with the explanation of the effect of the mean-velocity variations given in the preceding section, the neutral position for curve A at the peak is farther downstream than the neutral position for the corresponding curve at the valley. This corresponds to a 5.5-percent difference in boundary-layer thickness and is consistent with the mean-velocity data given in figure 10, which were obtained during the course of hot-wire measurements of the intensity. The averages of the initial values of $U/U_1$ were 0.38 and 0.36 for the peak and the valley, respectively, and these were used as the starting point for the Blasius curve shown in the figure. The actual points plotted in the figure, if carefully examined, indicate that there may be some decrease in velocity at the peak and some increase in velocity at the valley prior to breakdown. As will be seen, this effect is real but small (order of 10 percent) and is submerged in the scatter. Much of the scatter in the measured data can easily be due to small variations in position from the surface as the hot wire is moved downstream. Consequently the mean velocity at breakdown is shown departing from the Blasius curve. Observations of flow breakdown at a peak with a hot wire at $y = 0.12$ inch were in good agreement with this position. The point of departure of mean flow from the Blasius curve was used to specify the x-position of initial breakdown ocurring at the peak, and this is the point identified on the curves of figure 8. It should be made clear that the breaking points noted in the figure indicate the intensity of the wave at the $y = 0.046$ inch position when initial breakdown occurs in the outer region of the layer. It is not to be inferred that breakdown of the wave originates at this y-position. The corresponding values of $u'/U_1$, are essentially the same in each case; they are 7.3, 7.3, and 7.4 percent for input levels B, C, and D, respectively. After breakdown occurs at a peak, the intensity at both peak and valley continues to increase to a maximum and then subsides to the fully developed turbulent flow condition. The apparent trend of the maximum values of $u'/U_1$ was not always repeated and is believed to be due to unsteady flow conditions rather than to any intrinsic characteristic. The average maximum level of intensity is 14 percent for both peak and valley.

The mean velocity is apparently a more sensitive indicator as to when the fully developed turbulent state is reached than is the intensity. Figure 10 shows that fully developed turbulent flow is reached slightly farther downstream at the valley than at the peak. This is to be expected, since breakdown occurs at the peak and the rapid growth in the valley does not result in the characteristic breakdown into turbulent spots. The wave in the valley is disturbed by the neighboring flow at the peak, and turbulence sets in as the spot at the peak spreads into the valley.

The effect of wave amplitude on the amplification rate is more directly seen in figures 11 and 12, where the faired curves through the measured points of figures 8 and 9 are replotted relative to the initial level and the wave length of the oscillation. The wave length was obtained by the observation of Lissajou figures resulting from the hot-wire signal and the input signal to the ribbon as the distance downstream from the ribbon was varied. The wave length for the 145-cps wave was 1.46 inches. With increasing wave amplitude, departure from the linear amplification rate takes place progressively farther upstream, as illustrated by curves B, C, and D in figure 11. The value of $u'/U_1$ at which departure occurs is the same irrespective of initial level, and is 1.1 percent for curves B and C. The initial value of $u'/U_1$ for curve D is 1.2 percent, and the wave shows little evidence of following the linear amplification rate and has apparently already departed. After departure there is a very rapid growth of the wave and in a few wave lengths breakdown occurs. The growth of the wave in the valley exhibits a noticeably different behavior. The corresponding curves for the valley in figure 12 appear to depart at about the same position from the linear curve as those at the peak, or a little sooner, but after departure the trend is initially in the opposite direction, showing evidence of damping and a growth rate less than that for curve A. At a position somewhat upstream of that corresponding to breakdown at a peak the growth rate begins to increase again. The only effect of the initial ribbon amplitude is to move the point of departure and initial breakdown farther upstream with no significant change in wave behavior. The growth curves shown are believed to be typical of behavior at any peak and valley, the only difference being that for other peaks and valleys the x-position at which departure takes place may vary depending on the local linear amplification rates and the degree of irregularity between peak and valley.

A distinction usually made is that for free-stream disturbance levels larger than a few tenths of a percent Tollmien-Schlichting waves do not appear as part of the transition process and that transition is due to disturbances in the flow outside the boundary layer, as proposed by Taylor (ref. 11). Bennett (ref. 12) has shown that for a free-stream disturbance intensity of 0.42 percent Tollmien-Schlichting waves still play a role. An interesting implication of the wave behavior as outlined above is that the same basic mechanism still exists at considerably higher free-stream disturbance levels. If the effect of the free stream is considered to be one of providing a spectrum of disturbances for the boundary layer, then large free-stream disturbance levels of the order of magnitude shown by curve D of figure 8 would cause transition to occur so rapidly that it would appear to occur locally without depending on prior amplification of waves as part of the transition process. The randomness associated with transition and the presence in the free stream of disturbances with three times the root-mean-square value make it difficult to detect any waves.

It was at first thought that the spanwise variation in wave intensity illustrated in figure 3 was a consequence of the peak exhibiting a nonlinear effect sooner than the valley and that peak and valley behaved independently. However, it is evident from the growth curves that a more complex mechanism is present involving transfer of wave energy from one spanwise position to another. A further discussion of this effect and results to support this conclusion are given in the section Energy Transfer.

A more detailed picture of the spanwise variation and wave growth is shown in figure 13, where the intensity distribution across the boundary layer for both peak and valley are compared on a nondimensional basis at various positions along growth curve B of figure 11. The nondimensional distance $y/\delta$ is used, where $\delta$ at the peak is taken as

$$\delta = 5\sqrt{\frac{\nu x}{U_1}}$$

and $\delta$ at the valley was increased by 5.5 percent. The $180^\circ$ phase shift predicted by the Tollmien-Schlichting theory is shown at both peak and valley at 0.6 $\delta$, and although the distributions are somewhat distorted close to the wall, the distribution at the peak shows the characteristic maximum amplitude at $y/\delta = 0.2$. Just upstream from initial breakdown the maximum at the peak has moved out to 0.3 $\delta$, and the phase reversal position for the peak no longer coincides with that at the valley, having moved out to 0.7 $\delta$. The spanwise variation in intensity is not present all the way across the boundary layer. At the low amplitude level in the range of linear amplification there is a relatively small variation in the vicinity of the critical layer, from 0.1 $\delta$ to 0.25 $\delta$. Although the peak has not yet departed from its linear growth rate, the valley already has, and there is some indication of energy transfer already existing, which is not sufficient to significantly alter the growth rate at the peak. In fact, the growth of the wave at the peak for the two lower intensity distributions which are in the linear range is approximately constant across the boundary layer. As the wave intensifies, the difference between peak and valley increases in magnitude and extends over more and more of the boundary layer, until close to breakdown it exists from about 0.1 $\delta$ to 0.9 $\delta$.

It is evident that the departure from the linear amplification rate does not take place to the same degree across the entire boundary layer. This is graphically shown in figure 14, where the growth of the wave at a peak is shown at $y = 0.12$ inch and $y = 0.046$ inch for two input levels. These measurements were made at a time when the pre-existing mean-flow irregularities were somewhat different in magnitude than for the data of figures 8 and 9. Although the mean-flow irregularity remained fixed for long periods of time, it was not a controlled condition and was frequently checked to see that it did not change during a

sequence of measurements. Nevertheless, the behavior of the wave at $y = 0.046$ inch is similar to those previously shown with an intensity level at departure of 1.1 percent and an intensity level at breakdown of 7.4 percent. Close to the wall the wave practically follows the linear amplification rate until breakdown. It should be noted that the intensity distributions at a peak and a valley in figure 13 do not exhibit the small differences in intensity expected as a consequence of the difference in linear amplification rate due to the pre-existing mean-flow variations. Although these small differences may be obscured by the experimental uncertainty, there is, as shown in the section Energy Transfer, a compensating feature involving transfer of wave energy from peak to valley near the surface. The dashed portions of the curves in figures 13 and 14 are therefore drawn to indicate a possible real effect.

As shown in figure 10, the mean velocity at the peak increases after breakdown and has the characteristic approach to a fully developed turbulent flow usually observed with natural transition. However, in the present situation the transition region is quite well fixed and is of considerably shorter extent than that observed for natural transition at these Reynolds numbers. A markedly different effect takes place in the valley, where there is a substantial decrease in mean velocity preceding the rise to that characteristic of fully developed turbulent flow. As mentioned previously, small changes in velocity were indicated prior to breakdown. In order to determine the effect of wave amplitude on the mean-velocity profile and to eliminate the effect of changing $\delta$, mean-velocity distributions were measured with a hot wire at a distance 10 inches downstream from the ribbon at different intensity levels in the $y = 0.046$ inch position obtained by varying the ribbon amplitude. Figures 15(a) and 16(a) show the mean-velocity distribution at a peak and a valley, respectively, for intensity levels corresponding to those existing in the region before breakdown. They support the conclusion that the nonlinearity involving the interaction between the fluctuating shear stress $\rho\overline{uv}$ and the mean velocity that has usually been considered (refs. 13 and 14) does not appear to be the governing effect in the departure of the wave from the linear amplification rate. The behavior of the wave at peak and valley also supports this conclusion. In addition an estimate was made of the fluctuating shear stress at the point of departure, where the value of $u'/U_1$ is 1.1 percent by assuming that the shear correlation coefficient has the value of -0.18, as given by linear theory, and that $v' = 0.1\,u'$ with the result that the fluctuating shear stress is only 0.7 percent of the laminar shear at the wall. However, as can be seen from the results presented in the section Energy Transfer, these assumptions are questionable, and direct measurements of $v'$ and $\overline{uv}$ would be required to obtain an accurate estimate of their magnitude. Nevertheless, if the same assumptions are applied to the breakdown position, the fluctuating shear stress reaches a magnitude which is 30 percent of the laminar shear, and it would be expected

that some effect should be noticed. Approaching breakdown there is a noticeable effect on the mean-velocity profiles associated with wave amplitude, but it is difficult to interpret this as a nonlinear interaction between $\rho\overline{uv}$ and mean velocity inasmuch as the change in profile at the valley is in the opposite direction to that at the peak. The phenomenon is complicated by being three-dimensional, and it is felt that this is probably the important factor in the behavior observed. It is possible that the changes observed in the mean-velocity profile at peak and valley with increasing wave amplitude result from the superposition of a vortex pattern associated with the wave motion. The velocity profile at a peak tends toward an unstable type in that it exhibits an inflection point, while at the valley the profile tends to become more convex. Consequently, these changes in profile shape may play an important role in the local amplification at peak and valley.



Attempts were made to measure changes in spanwise mean-flow direction in the region prior to breakdown with a V-wire arrangement which is admittedly not too accurate for small angle changes. Variations of the order of $1^{\circ}$ were observed in the mean-flow direction without the wave present. These were consistent with the weak longitudinal vortex picture of the mean-velocity variations. Small-amplitude waves had no effect on these small variations in direction. With large-amplitude waves, variation occurred in the directional pattern, but these variations were no larger than those pre-existing in the flow and consequently were difficult to interpret.

Figures 15(b) and 16(b) show the mean-velocity distributions for intensity levels in the region from breakdown to fully developed turbulent flow. The distributions for the different intensity levels are consistent with the results represented by curve C in figures 8 and 10, and from these the corresponding x-positions in the transition region can be obtained. The distributions in the valley exhibit the initial defect in velocity which occurs after breakdown at the peak and then show the change in profile toward a fully developed turbulent distribution as the spot at the peak spreads into the valley. In natural transition with large transition regions the randomness in spot origin produces a superposition of effects, giving the impression of alternating laminar and turbulent flow characterized by an intermittency factor. The manner in which the change to a turbulent profile takes place when there is a regular succession of spots in a fixed street is shown in figure 15(b). The phenomenon is characteristic of a streetlike array of a train of spots in an early stage of development, not of the single fully developed turbulent spot as studied in reference 2. It is now apparent that the change from a laminar to a turbulent profile is closely connected with the development of turbulent spots. It is seen that large changes in mean velocity are associated with breakdown of the wave. However, at this stage of the investigation it is not known which is

the primary factor in the transition process. Are the changes in mean velocity a later stage of the small changes noted prior to breakdown, or does this behavior of the mean velocity result from breakdown? An understanding of the changes that take place in the mean flow both before and after breakdown is an important consideration in the mechanism of transition and warrants further investigation. In the region from breakdown to where the intensity reaches a maximum the mean-velocity profiles show little evidence of thickening. All of the velocity change takes place on the wall side of the phase reversal point.



Several investigators of transition in supersonic boundary layers (refs. 15 to 17) have observed that photographic methods, such as schlieren and shadowgraph, locate transition at a position farther downstream than do surface-temperature measurements. On the basis of present observations a possible explanation for this effect is that the schlieren technique is not sensitive to the initial breakdown, which, as is shown in the section Wave Breakdown, is initially of smaller scale than the boundary-layer thickness. It will reflect only a later stage of the transition process where the density gradients become sufficiently intense, as would be expected in the vicinity of maximum u', and where there is a substantial thickening of the layer. On the other hand, surface-temperature measurements will be sensitive to the initial breakdown and the accompanying mean-velocity change. It may be that the overshoot observed with surface-temperature measurements is related to the maximum intensity levels of figure 8.

Since the effect of frequency was to shift the peaks and valleys of the wave relative to the pre-existing mean-flow variations, measurements similar to those made for the 145-cps wave were also made for a 70-cps wave which lies near branch I of the stability diagram and which had a wave length of 2.7 inches. The values of $\beta_r \nu / U_1^2$ are $29 \times 10^{-6}$ and $60 \times 10^{-6}$ for the 70- and 145-cps waves, respectively. This afforded the possibility of isolating those features of the phenomenon which accompany the wave. In the case of the 70-cps wave it was possible to observe the wave behavior for longer distances from the vibrating ribbon with a greater extent of the linear range, since branch II of the stability diagram and the subsequent damping region are at an appreciable distance downstream. Figures 17 and 18 show the growth in intensity at a fixed distance from the wall, y = 0.046 inch, for the 70-cps wave at a peak for different input levels of the vibrating ribbon. The accompanying mean-velocity data are shown in figure 19. An oscillogram showing the breaking pattern observed for the 70-cps wave is also shown in figure 17. Although the peak for the 70-cps wave is interchanged with the valley for the 145-cps wave, behavior similar to that for the peak of the 145-cps wave is observed. Corresponding measurements of the growth in intensity at a neighboring valley for the 70-cps wave were not made. However, the intensity distributions across the boundary layer for a

peak and a valley at different downstream positions of the growth curve G are shown in figure 20, and it is seen that in the valley the 70-cps wave exhibits the same lack of growth as observed for the 145-cps wave. The intensity distributions at the peak are quite similar in shape to those for the 145-cps wave at a peak, but at the valley their shape in the vicinity of the critical layer is somewhat different. It is not known to what extent the pre-existing mean-flow variations influence these details. Nevertheless the distributions exhibit the same characteristic increase in magnitude and increasing extension across the boundary layer of the difference between peak and valley as the wave intensifies. The phase reversal is now seen to occur at 0.7 $\delta$ as contrasted with 0.6 $\delta$ for the 145-cps wave. The same trend is also noticed in the Tollmien-Schlichting amplitude distribution for neutral waves on branches I and II of the stability diagram. The pertinent information with respect to the growth curves at a peak for both the 70- and 145-cps waves is summarized and compared in the following tables. It should be stressed that the comparison is obtained for a fixed distance from the wall at $y = 0.046$ inch in the vicinity of the maximum in the amplitude distribution across the boundary layer.

| Input level | Wave frequency, cps | $\frac{u'}{U_1}$ at departure | $\frac{u'}{U_1}$ at breakdown | Distance from departure to breakdown, in. |
|---|---|---|---|---|
| B | 145 | 0.011 | 0.073 | 6.1 |
| C | 145 | .011 | .073 | 5.4 |
| D | 145 | ----- | .074 | --- |
| Average | 145 | .011 | .073 | 5.8 |
| F | 70 | 0.021 | 0.075 | 7 |
| G | 70 | .021 | .067 | 6 |
| Average | 70 | .021 | .071 | 6.5 |

| Input level | Wave frequency, cps | Distance from breakdown to maximum $u'/U_1$, in. | Maximum $u'/U_1$ | Extent of transition region, in. |
|---|---|---|---|---|
| B | 145 | 4.4 | 0.16 | 9 |
| C | 145 | 3.7 | .14 | 8 |
| D | 145 | 4.0 | .13 | 8 |
| Average | 145 | 4.0 | .14 | 8.3 |
| F | 70 | 6.0 | 0.14 | 11 |
| G | 70 | 6.5 | .12 | 10 |
| Average | 70 | 6.3 | .13 | 10.5 |

The $Re_{\delta^*}$ at breakdown for the 70- and 145-cps waves ranged from 1750 to 2020, and the flow conditions have not been sufficiently varied to evaluate the significance of their having the same intensity at breakdown. The difference in intensity level at departure is proportional to the wave length, but here again it is difficult to evaluate its significance. It is felt that this difference reflects the degree of irregularity rather than the effect of wave length. The 70-cps wave has initially less spanwise variation in intensity than does the 145-cps wave, and from figures 13 and 20 it can be seen that at departure they are about the same. Accordingly it appears that the departure is probably a manifestation of the strength and subsequent nonlinearity of the three-dimensional wave. The distance from departure to breakdown is independent of wave length; so also is the maximum intensity independent of wave length. An interesting feature of the comparison is the longer extent of the transition region for the 70-cps wave than for the 145-cps wave. Within the experimental accuracy the difference is a little less than twice the difference in their wave lengths. All of the difference takes place in the region where the intensity after breakdown increases to a maximum. This is consistent with observations made in the section Wave Breakdown that this region is associated with the distance in which a succession of turbulent bursts overtake one another. The decrease in intensity from a maximum to a value characteristic of fully developed turbulent flow is independent of wave length, and in this region diffusion as well as a redistribution of energy spectrally and among the various components probably takes place.

An important aspect of the wave development is the question as to whether there are distortions in the wave front accompanying the spanwise variations in amplitude. In figures 21 and 22 representative records of the u-fluctuation of the 145-cps wave at varying positions across the boundary layer for peak and valley, respectively, are compared with the input signal to the ribbon as a reference. The top trace in each of the oscillograms is the reference signal. The intensities at the respective positions are noted in the figures and are of a magnitude existing prior to breakdown corresponding to the intensity distributions farthest downstream at peak and valley shown in figure 13. At a peak there is no change in phase of the wave across the boundary layer except for the expected Tollmien-Schlichting $180^\circ$ phase shift near the outer edge. In the valley the wave exhibits a peculiarly different and not too well understood behavior. In a restricted region of the layer, as illustrated by the records at $y = 0.04$ inch and $y = 0.06$ inch, there is a marked distortion of the wave with an apparent $180^\circ$ phase shift. Close to the wall and in the outer region of the layer the wave is essentially in phase with that at the peak and also shows the customary phase reversal near the outer edge. It is not to be inferred that a $360^\circ$ phase shift takes place across this narrow region in the valley. Very close to breakdown measurements of wave velocity, wave length, and phase were uncertain, but as far as could be determined the

wave at peak and valley, except for this narrow region in the valley, traveled downstream with a wave velocity and a wave length given by the Tollmien-Schlichting theory practically up to the breaking point with no significant spanwise distortion in the wave front. The unusual phase shift in the valley appeared to be the result of a progressive change in the downstream direction which had its beginning at about the point where the wave departed from the linear amplification rate. It manifested itself as a change in wave length and wave velocity which in a downstream direction increased to a maximum and then decreased to the original Tollmien-Schlichting values with no subsequent change and a resulting $180^{\circ}$ phase shift. The physical significance of an increasing and then decreasing wave velocity in a restricted region of the boundary is rather obscure, and it is felt that the behavior observed is a result of changes in wave shape due to harmonic distortion rather than a distortion of the wave front. Furthermore no such behavior was observed with the 70-cps wave. It is concluded therefore that no shape distortion in the wave front takes place prior to breakdown and that the wave lengths and wave velocities are adequately given by the Tollmien-Schlichting theory. In this connection it should be mentioned that Fales and Hama, Long, and Hegarty (refs. 18 and 19) have conducted investigations in water of transition on a flat plate behind a trip wire using dye techniques and have observed that the vortices shed by the trip wire became strongly three-dimensional prior to transition. The results of Hama, Long, and Hegarty bear certain similarities to those of the present investigation in that they show not only the rapidity with which breakdown occurs once the three-dimensionality is evident, but also the streetlike succession of turbulent bursts with breakdown occurring near the outer edge of the layer. On the other hand, the variations in wave velocity and distortion of the wave front corresponding to the vortex loop formation shown by the dye technique are not observed prior to breakdown. If, as proposed by Hama et al, the Tollmien-Schlichting waves concentrate into discrete vortices and the dye remains with the wave, large changes in wave velocity should be present. However, no significant changes in wave velocity occur prior to breakdown which would give the large deformations they observed. It is apparent that the dye technique marks the fluid particle and thus shows the behavior of the mean flow but not necessarily that of the wave. It is only after initial breakdown that large spanwise variations in mean velocity have been observed which are sufficient to deform a line of dye into a strong loop configuration. It may be speculated that the breakdown observed by Hama et al reflects a later stage of the breakdown process where the motions become strongly diffusive and that the line of dye is not sensitive to the initial small-scale breakdown. Another speculation is that the motions associated with the three-dimensional wave in some manner would give rise to a displacement of the dye in and out from the surface at different spanwise positions with a resulting loop configuration. The foregoing speculations attempt to reconcile the difference between the results of Hama et al and those of the present investigation on the assumption that the difference lies in

the method of observation and not in the phenomena. An interesting speculation by Schubauer (ref. 8) is that the phenomena are basically different. He suggests that the disturbance introduced by the vibrating ribbon is much weaker than the discrete vortices introduced by the trip wire and that the transition occurs, because of the higher Reynolds numbers of the present investigation, before the relatively weaker wave can concentrate the vorticity into discrete eddies. At an early stage of the investigation a few preliminary measurements were made downstream of a 1-millimeter trip wire, and these showed the existence of spanwise variations in intensity. However, the measurements were not systematic enough at the time to make further comparison with the water experiments. It may well be that a more thorough and systematic investigation of transition behind a trip wire using hot-wire techniques would be helpful in resolving the question as to whether the difference noted is due to the method of observation or an actual difference in phenomena.

## Energy Transfer

It has been inferred from the behavior of the growth curves as outlined in the previous section that energy is being transferred from one spanwise position to another. The existence of a mean-energy transfer associated with the wave is shown by figures 23 and 24. The rate at which energy is being transferred in the spanwise direction $\overline{wu^2}$ is plotted nondimensionally with respect to the free-stream mean velocity. The corresponding u and w intensities are also given. The measurements were made at a distance of 7 inches downstream from the vibrating ribbon at 0.046 inch from the surface. The difference in intensity level shown in figures 23 and 24 was obtained by varying the ribbon amplitude; however, both levels are of such magnitude that they can be interpreted as corresponding to two different downstream positions in the region from departure to breakdown. The arrows indicate the direction in which energy is being transferred, a negative gradient indicating a gain of energy and a positive gradient a loss of energy. The measurements are quite difficult and there is appreciable scatter but the trend is apparent. It is seen that the peaks are gaining energy and the valleys are losing energy, where peaks and valleys are defined by the spanwise variation in intensity of the u-fluctuation. Consequently there is an energy-concentrating mechanism present which concentrates the energy at a peak and depletes it at a valley. At low wave amplitudes corresponding to the range before departure no significant energy transfer could be measured, and if any was present it was submerged in the experimental uncertainty.

Measurements of the correlation between the u- and w-fluctuations across the boundary layer were made at $z = 2.1$ and $z = 2.5$ inches, corresponding to spanwise positions where the energy transfer is in

opposite directions, and these are shown in figures 25 and 26. Two correlation curves are shown at each position, and these were obtained for two waves of different amplitudes, a wave of low amplitude of magnitude existing in the range before departure from the linear amplification rate, and the other of magnitude existing in the range from departure to breakdown. The Roman numerals are used to identify the correlation curves with their respective distributions of $u'$ and $w'$ given in figures 27 and 28. It is seen that for the low-amplitude wave the same basic correlation between $u$ and $w$ exists. The existence of a u- and w-correlation does not of itself constitute a nonlinear mechanism resulting in the energy transfer. It is difficult to gain an insight by assessing and comparing the distributions of $u'$ and $w'$. Their relation to one another no doubt varies with spanwise position, and their study would involve considerable detailed measurement. However, they do show a strong intensification of the three-dimensionality, as evidenced by the growth in $w'$. It is interesting to note that the distribution of $w'$ shows a maximum in the vicinity of the critical layer and that the magnitude of $w'$ has its greatest variation on the wall side of the phase reversal position of $u'$, corresponding to the region where the spanwise variation in $u'$ for peak and valley is predominant. The rate of energy transfer shown in figure 24 is about a factor of 10 less than that for the higher intensity wave shown in figure 23, which also indicates a strong intensification of the energy-concentrating mechanism in the region from departure to breakdown.

The fact that the spanwise distribution of $w'$ shown in figures 23 and 24 have their maximum between peaks and valleys of the spanwise variation in $u'$ and the nature of the energy transfer itself are a good indication that longitudinal vortices accompanying the wave may be present in the flow. The nature of the correlation between $u$ and $w$ indicates a much more complex system of vortices than a simple circulatory disturbance. The shift in the correlation curve at the higher amplitude is probably associated with the behavior of the $u'$-distributions at a peak and valley previously discussed in connection with figure 13. Representative oscillograms of the simultaneous u- and w-fluctuations at different positions across the boundary layer for the $z = 2.1$ inch and $z = 2.5$ inch positions are shown in figures 29 and 30, respectively. The amplification was adjusted at each position so that the traces would show to the best advantage, and no significance should be attached to the relative amplitude of the fluctuations as shown in the records. They were obtained for an arbitrary wave amplitude in the region from departure to breakdown, and consequently the phase between the u- and w-fluctuations illustrated by the oscillograms for a given position in the boundary layer does not necessarily correspond with the correlation curves. Except for the shift with increasing amplitude, the correlation curves do not change significantly with respect to the phase relations involved, and in this respect the oscillograms should be consistent with the measured correlation.

Because of the dynamic character of the motion, it would not be expected that the measured mean values of the correlation correspond exactly to the relative phases of the instantaneous u- and w-fluctuations shown by the oscillograms, and it may be inferred that the high degree of correlation measured, for example at the maximum and minimum of figure 25, reflects a correlation of +1 and -1 in the basic phenomenon. This is especially true near the surface, where the records at $y = 0.01$ inch and $y = 0.024$ inch in figures 29 and 30, respectively, show variation in phase between u and w with time. The w-fluctuation in the oscillogram at $y = 0.01$ inch of figure 29 varies from in phase to out of phase relative to u and tends to undergo frequency doubling. At the $y = 0.024$ inch position of figure 30, sizeable phase variation between u and w with time are also evident. Consequently no phase angles for these two positions are noted in the figures. At other positions in the boundary layer the phase relations were much steadier with time. The w-fluctuation is leading in phase with an increasing phase angle across the boundary layer and near the edge of the boundary layer has advanced in phase $540^{\circ}$ relative to the u-fluctuation at the $z = 2.1$ inch position. At the $z = 2.5$ inch position the w-fluctuation is also leading in phase with an increasing phase angle across the boundary layer, but at the edge of the layer it has advanced in phase relative to the u-fluctuation only $270^{\circ}$. In general these phase changes are of a magnitude consistent with those indicated by the correlation curves.

The inference drawn from comparison of the correlation curves at the $z = 2.1$ inch and $z = 2.5$ inch positions, that near the surface energy transfer in the opposite direction takes place, was substantiated by spanwise measurement of $\overline{wu^2}$ at $y = 0.015$ inch. The input level of the ribbon was adjusted to give the u-intensity shown in figure 23, and in figure 31 the spanwise distribution of $\overline{wu^2}$ obtained at $y = 0.015$ inch is compared with the corresponding distribution at $y = 0.046$ inch. It is seen that the transfer is in the opposite direction and that the rate at which energy is being transferred is of considerably smaller magnitude. An attempt was made to measure the spanwise distribution of $\overline{wu^2}$ at $y = 0.12$ inch, which corresponds to about 0.6 $\delta$, but within the experimental accuracy no significant energy transfer could be detected. Here again, it is interesting to note that the significant energy transfer appears to be located on the wall side of the phase reversal point in u', corresponding to the region where the spanwise variation in u' for peak and valley is predominant. It was intuitively expected that the correlations at the $z = 2.1$ inch and $z = 2.5$ inch positions might be mirror images of one another. The fact that this is not completely borne out by observations makes the mechanics involved in the phase relations somewhat obscure. There possibly exist multiple vortices, and the mean flow may play a role in characterizing the behavior. Within the region from approximately 0.05 $\delta$ to 0.5 $\delta$ the correlations do

present a mirror image of one another while going through a 180° phase change, which indicates the possible existence of a pair of counter-rotating longitudinal vortices within this region, with their centers on each side of the peak in the spanwise distribution of u'.

The issue is complicated by the existence of the pre-existing mean-flow variations. However, survey measurements of the energy transfer and correlation of the u- and w-fluctuations for the 70-cps wave showed the same behavior. It will be recalled that the effect of wave length was to shift the three-dimensionality of the wave relative to the mean-flow variations, and since the essential features accompanying the growth of the wave remained the same, indications favor the point of view that the phenomena observed are an inherent characteristic of the wave development rather than a direct manifestation of the pre-existing mean-flow variations. The question as to whether a two-dimensional wave can lead to transition may be academic. It is possible that any small irregularity may trigger the phenomenon herein described, and it does not appear likely that a purely two-dimensional wave can be maintained experimentally. It can perhaps be speculated that a purely two-dimensional wave would not lead to transition.



An important question in connection with the possible existence of longitudinal vortices is that pertaining to their originating mechanism. Görtler (ref. 20) has suggested the concept of a secondary instability, in that the concave streamline curvature associated with the wave motion may generate vortices with axis alined along the flow. It has been informally reported to the authors that Görtler and Witting (ref. 21) have proposed that such an instability may occur when the parameter $\left(\frac{U_1}{\nu}\right)^2 \frac{\delta^{*3}}{r}$ has a value of about 11, where $r$ is the minimum value of the streamline radius of curvature within the boundary layer and the corresponding streamline displacement is of the order of $\delta^* \times 10^{-4}$. Values of the streamline displacement and streamline radius of curvature pertaining to the point of departure from the linear amplification rate at a peak for the 145- and 70-cps waves are shown in figure 32. These were calculated on the basis of a sinusoidal wave from the mean-velocity distribution and measured u-intensity distribution at the point of departure. The values of the maximum streamline displacement are $0.02\ \delta^*$ and $0.04\ \delta^*$ for the 145- and 70-cps waves, respectively, and the corresponding values of the Görtler-Witting parameter are 5140 and 4220. These values are of a much higher order of magnitude than those proposed by Görtler and Witting. It is evident that their criterion would involve quite small amplitudes with the result that the secondary instability could be considered to be practically an inherent characteristic of the wave and already existing at the initial input levels of the vibrating ribbon. The Görtler-Witting paper is not available to the authors at this writing, and it is difficult to evaluate the validity of their concept on the basis of the present experimental evidence. The correlations

between the u- and w-fluctuations would tend to indicate a different originating mechanism, but these are not understood well enough at present to draw any final conclusions. By way of conjecture, another mechanism which is suggested by the experimental evidence is that a wave of varying spanwise amplitude in a shear flow, with a wave velocity which for the greater portion of the boundary layer is less than that of the mean velocity, would of itself tend to generate a complex system of longitudinal vortices. Thus the irregularity rather than the streamline curvature is the controlling feature.



## Wave Breakdown

The streetlike configuration of transition resulting from breakdown at the peak positions in the spanwise distribution of wave intensity was made visible by means of the China-clay technique. A typical pattern is shown in figure 33. A section of the surface, 1 foot in width, was coated with a thin layer of China clay, which was then sprayed with oil of wintergreen. Waves were produced with the vibrating ribbon, and after a running time of 20 minutes the drying pattern shown was obtained. The dark line at the left of the figure is the vibrating ribbon which appears slanted because of the angle at which the picture was taken. The white streaks show the regions of breakdown. The limitations of the method prevent drawing any conclusions as to the existence of longitudinal vortices in the region before breakdown. As far as could be determined, the beginning of the white streaks coincides with the initial breakdown of laminar flow and the associated large spanwise variations in mean velocity.

The breakdown of the wave as detected by a hot wire sensitive to the u-fluctuation, and which has already been briefly alluded to, is illustrated in more detail in figure 34. The oscillograms shown in the figure which are representative of the breakdown process were not obtained by moving the hot-wire probe through the transition region but by moving the transition region over the hot-wire probe by continuously increasing the ribbon amplitude. The records were obtained at a position corresponding to a peak in the spanwise distribution of $u'$, and at a position 0.12 inch from the surface.

The amplifier gain was kept fixed for the full range of conditions and was set to keep the higher intensity traces on the film. As a result the first record appears as little more than a wavy line. In this record a characteristic distortion has already set in, namely, a flattening of the high-velocity side and a sharpening of the low-velocity side. As the forcing amplitude is increased, there develop next, somewhat sporadically and suddenly, intense low-velocity spikes. These spikes then increase in number and form bunches of high-frequency

fluctuations which follow one another in succession once each cyle of the primary wave, and when they have covered 1 wave length they have caught up with one another. The occurrence of the single low-velocity spike was taken as an indication of initial breakdown. The abruptness and high intensity with which this phenomenon appears marks it as something apart from a developing distortion of the primary wave. It is therefore termed a "breakdown" of the laminar flow. This is in marked contrast to the transition phenomenon in a pipe studied by Leite (ref. 22) in which transition resulting from large induced disturbances was observed to take place gradually.



In order to determine the location and extent of the initial breakdown, oscillograms of simultaneous signals from two hot wires sensitive to u-fluctuations were obtained when in one case the wires were separated in the z-direction and in another when they were separated in the y-direction. The first case is shown in figure 35, and the second is shown in figure 36. The lower record in each oscillogram of figure 35 represents the signal from a hot-wire probe which was kept fixed at a z-position corresponding to a peak in the spanwise variation of $u'$ and shows the characteristic breaking pattern with which the simultaneous signal from a hot-wire probe displaced different amounts in the z-direction is compared. Both hot-wire probes were at 0.12 inch from the surface. With a separation of 0.1 inch the signal from the hot-wire probe which is displaced from the peak shows a fluctuation somewhat regular in character on the high-velocity side of the wave and of much smaller intensity than at the peak. As the separation is increased, the fluctuation from the displaced probe decreases and for a separation of 0.4 inch it has disappeared. The oscillograms in figure 36 show the simultaneous signals from two hot-wire probes displaced in the y-direction. One of the oscillograms compares the fluctuation at the $y = 0.12$ inch position with that obtained from a probe displaced 0.11 inch toward the surface, and the other shows the comparison for a displacement of 0.11 inch toward the outer edge of the layer. The flow at the displaced positions is disturbed but does not show the characteristic behavior of the breaking pattern. It is inferred from the nature of the oscillograms that the disturbances at the displaced positions in $y$ and $z$ are pressure-caused excitations transmitted from the intense disturbance at the peak, and that the initial breakdown itself is highly localized. It is difficult to specify a region distinct from the disturbance it creates. However, visual observation of the breaking pattern for the 145-cps wave at the stage of the breakdown shown in figures 35 and 36 indicated that the extent of the intense low-velocity spiked appearance typical of a breaking pattern was about 0.25 $\delta$ in the y-direction and occupied the region from 0.5 $\delta$ to 0.75 $\delta$. The extent in the z-direction was somewhat larger, being about 0.75 $\delta$. Visual observation also indicated that in the initial stages of breakdown the breaking pattern is not very diffusive. Consequently it is felt, at least at this stage of

the investigation, that the large changes in mean velocity associated with the initial stages of breakdown discussed previously in the section Wave Growth and Effect on Mean Flow do not result from turbulent momentum transfer in the usual sense.

It is evident from the fact that the breaking patterns overtake one another that the downstream end must be traveling faster than the upstream end. A measure of the velocities associated with the breaking pattern was obtained by observing the simultaneous signals from two hot wires separated longitudinally by a distance of 0.52 inch with one wire directly behind the other. Interference was avoided by making the upstream wire longer than the downstream wire and by using very fine prongs. Both wires were at a peak position and 0.12 inch from the surface. Oscillograms (a) and (b) of figure 37 show representative samples of the records obtained, oscillogram (b) corresponding to a little later stage of the breakdown process than oscillogram (a). In order to obtain adequate resolution, film speeds of 30 to 35 feet per second were used for records (a) and (b). It should be pointed out that only for oscillograms (a) and (b) of figure 37 is decreasing velocity upward toward the timing signal. In all the other oscillograms increasing velocity is downward toward the timing signal. However, time is increasing from right to left for all oscillograms. It is seen that the breaking pattern arrives first at the upstream wire and then a short time later at the downstream wire, and that it departs first at the upstream wire and later at the downstream wire. The short vertical lines shown on the oscillograms identify that portion of the trace which was taken as the beginning and end of a breaking pattern, and from the time delay the velocities of the upstream and downstream ends were calculated. The average values obtained from the inspection of a number of such records were 18 feet per second for the upstream end and 41 feet per second for the downstream end. These values correspond closely to the wave velocity and local mean velocity in the boundary layer, respectively. It is apparent that, with the upstream end traveling with the wave velocity, a breaking pattern will overtake a previous one when it has occupied 1 wave length of the primary wave. The distance along the surface for them to overtake one another depends on the velocity of the downstream end, and it is possible that this may vary to some degree across the y-extent of the breaking pattern. However, if the value of 41 feet per second is taken as being fairly representative of the velocity of the downstream end for both the 145- and 70-cps waves, then using the appropriate values of the wave velocity for the upstream end, it is estimated that the breaking patterns overtake one another in 2.6 and 4.4 inches for the 145- and 70-cps waves, respectively. These values apply for a free-stream velocity of 50 feet per second.

An interesting question in connection with breakdown of the flow is whether or not intermittent flow separation occurs. The excursions to

lower velocity making up the breaking pattern, which are still relatively small compared with the local mean velocity, are confined to the outer region of the layer. This is shown by oscillogram (c) of figure 37, which compares simultaneous u-signals from two hot wires, one 0.005 inch and the other 0.12 inch from the surface, both located at the initial stage of breakdown. Although the initial spike occurs while the velocity at the surface is decreasing, there is no evidence that separation occurs. The intensity of the u-fluctuation at $y = 0.005$ inch is only about 20 percent of the local mean velocity, and the wave does not exhibit any skewness which would be sufficient to indicate momentary separation. Thus it is felt that in the case of zero pressure gradient intermittent separation does not accompany transition.



In view of the information obtained on the wave development and breakdown, it was of interest to see whether characteristic breakdown patterns could be observed in the case of natural transition, that is, that resulting from the random disturbances in the wind tunnel and without artificial excitation, as by a vibrating ribbon. In this case the waves appear highly modulated; transition is not well fixed, and the transition region is of relatively long extent. However, since the frequency selected for amplification in natural transition generally lies near branch II of the stability diagram, it is not surprising that on the average the existence of spanwise variations in wave intensity in line with the pre-existing mean-flow irregularities was observed. A hot wire sensitive to the u-fluctuation was placed at a z-position of higher velocity in the pre-existing spatial mean-flow irregularity and was positioned at $y/\delta = 0.6$ and at an x-position corresponding to the observed beginning of the transition region. In figure 38 the oscillograms obtained are shown; it can be seen that intermittently the same characteristic breakdown patterns do occur.

## CONCLUSIONS

This investigation dealt with the case where waves originating by laws of small-perturbation theory are the agents which bring about transition. This case does not cover all transition-producing situations, but it does cover situations where significant amounts of laminar flow may be expected, and basically those cases where stability theory is applicable.

A definite and reproducible progression of events was found by which a wave disturbance evolves into turbulent flow, of which the essential features are as follows:

1. The wave motions become strongly three-dimensional prior to transition.

2. Accompanying the wave motion there is present an energy-concentrating mechanism involving the transfer of wave energy from one spanwise position to another. There is evidence that associated with this energy-concentrating mechanism there are longitudinal vortices.

3. The breakdown of laminar flow occurs in the regions of energy concentration.

4. The initial breakdown of laminar flow occurs in the outer region of the boundary layer and is of such small extent that it may be loosely described as pointlike.

5. The local regions of breakdown are the initial stages in the development of turbulent spots.

6. Intermittent separation is not a factor in the transition of a laminar boundary layer with zero pressure gradient.

National Bureau of Standards,
Washington, D. C., February 1, 1958.

## REFERENCES

1. Laufer, John, and Vrebalovich, Thomas: Experiments on the Instability of a Supersonic Boundary Layer. EP 350, Jet Prop. Lab., C.I.T., Aug. 27, 1956.

2. Schubauer, G. B., and Klebanoff, P. S.: Contributions on the Mechanics of Boundary-Layer Transition. NACA Rep. 1289, 1956. (Supersedes NACA TN 3489.)

3. Emmons, H. W.: The Laminar-Turbulent Transition in a Boundary Layer, pt. I. Jour. Aero. Sci., vol. 18, no. 7, July 1951, pp. 490-498.

4. Schubauer, G. B., and Skramstad, H. K.: Laminar Boundary-Layer Oscillations and Transition on a Flat Plate. NACA Rep. 909, 1948. (Supersedes NACA WR W-8.)

5. Tollmien, W.: The Production of Turbulence. NACA TM 609, 1931.

6. Schlichting, H.: Zur Entstehung der Turbulenz bei der Plattenstromung. Nachr. Ges. Wiss. Gottingen, Math. Phys. Klasse, 1933, pp. 181-208.

7. Schlichting, H.: Amplitude Distribution and Energy Balance of Small Disturbances in Plate Flow. NACA TM 1265, 1950.

8. Schubauer, G. B.: Mechanism of Transition at Subsonic Speeds. Boundary Layer Res., Proc. Int. Union and Appl. Mech., H. Görtler, ed., Springer Verlag (Berlin), 1958, pp. 85-108.

9. Kovásznay, Leslie S. G.: Development of Turbulence-Measuring Equipment. NACA Rep. 1209, 1954. (Supersedes NACA TN 2839.)

10. Schubauer, G. B., and Klebanoff, P. S.: Theory and Application of Hot-Wire Instruments in the Investigation of Turbulent Boundary Layers. NACA WR-W-86, 1946. (Supersedes NACA ACR 5K27.)

11. Taylor, G. I.: Statistical Theory of Turbulence. V - Effect of Turbulence on Boundary Layer. Proc. Roy. Soc. (London), ser. A, vol. 156, no. A888, Aug. 17, 1936, pp. 307-317.

12. Bennett, H. W.: An Experimental Study of Boundary-Layer Transition. Kimberly-Clark Corp., Sept. 1953.

13. Liepmann, H. W.: Investigations of Boundary Layer Transition on Concave Walls. NACA WR W-87, 1945. (Supersedes NACA ACR 4J28.)

14. Stuart, J. T.: On the Effects of the Reynolds Stress on Hydrodynamic Stability. Z.A.M.M. (Sonderheft), 1956, pp. S32-S38.

15. Laufer, John, and Marte, Jack E.: Results and a Critical Discussion of Transition-Reynolds-Number Measurements on Insulated Cones and Flat Plates in Supersonic Wind Tunnels. Rep. No. 20-96 Jet Prop. Lab., C.I.T., Nov. 30, 1955. (Contract DA-04-Ord 18.)

16. Brinich, Paul F.: Boundary-Layer Transition at Mach 3.12 With and Without Single Roughness Elements. NACA TN 3267, 1954.

17. van Driest, E. R., and Boison, J. C.: Experiments on Boundary-Layer Transition at Supersonic Speeds. Jour. Aero. Sci., vol. 24, no. 12, Dec. 1957, pp. 885-899.

18. Fales, Elisha N.: A New Laboratory Technique for Investigation of the Origin of Fluid Turbulence. Jour. Franklin Inst., vol. 259, no. 6, June 1955, pp. 491-515.

19. Hama, F. R., Long, J. D., and Hegarty, J. C.: On Transition from Laminar to Turbulent Flow. Jour. Appl. Phys., vol. 28, no. 4, Apr. 1957, pp. 388-394.

20. Görtler, H.: Dreidimensionale Instabilität der ebenen Staupunktströmung gegenüber wirbelartigen Störungen. 50 Jahre Grenzschichtforschung Friedr., Vieweg & Sohn, 1955, pp. 304-314.

21. Gortler, H., and Witting, H.: Theorie der sekundären Instabilität der laminaren Grenzschicten. Boundary Layer Res., Proc. Int. Union and Appl. Mech., H. Görtler, ed., Springer Verlag (Berlin), 1958, pp. 110-126.

22. Leite, Richard J.: An Experimental Investigation of the Stability of Axially Symmetric Poiseuille Flow. TR 56-2, Eng. Res. Inst., Univ. Mich., 1955.

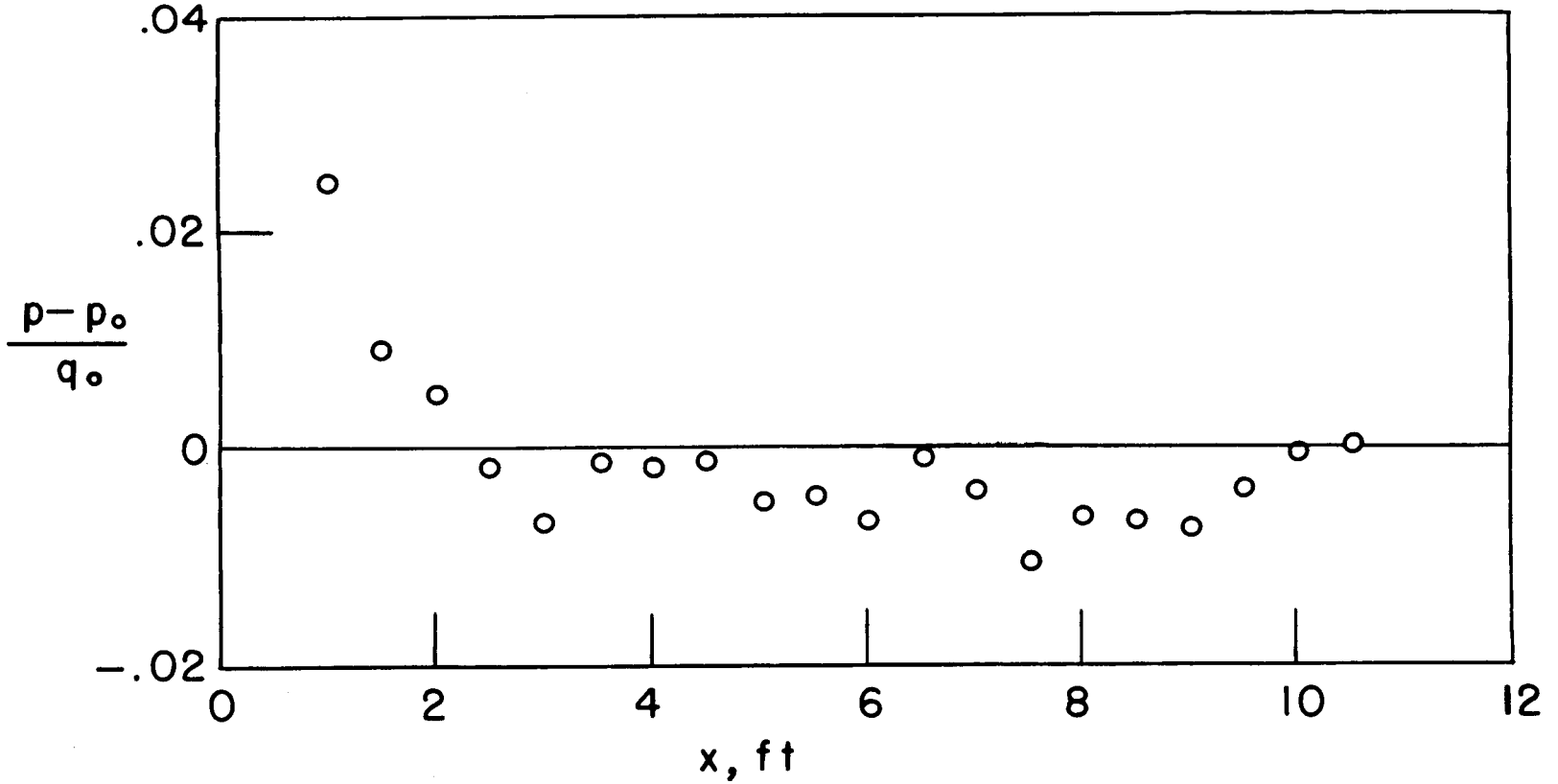


Figure 1. - Pressure distribution along flat plate.

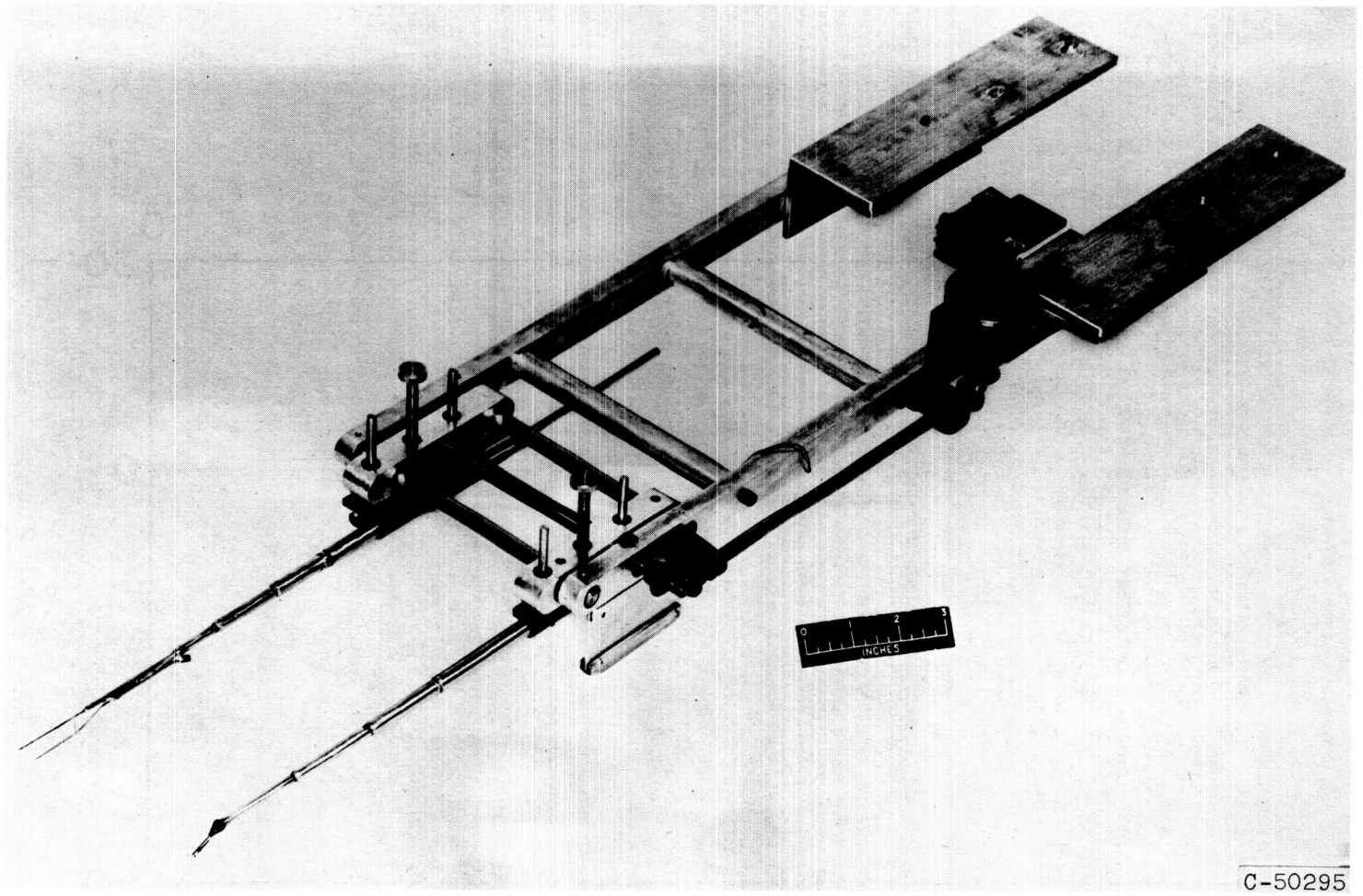


Figure 2. - Traversing mechanism with pitot-static arrangement and hot-wire probe attached.

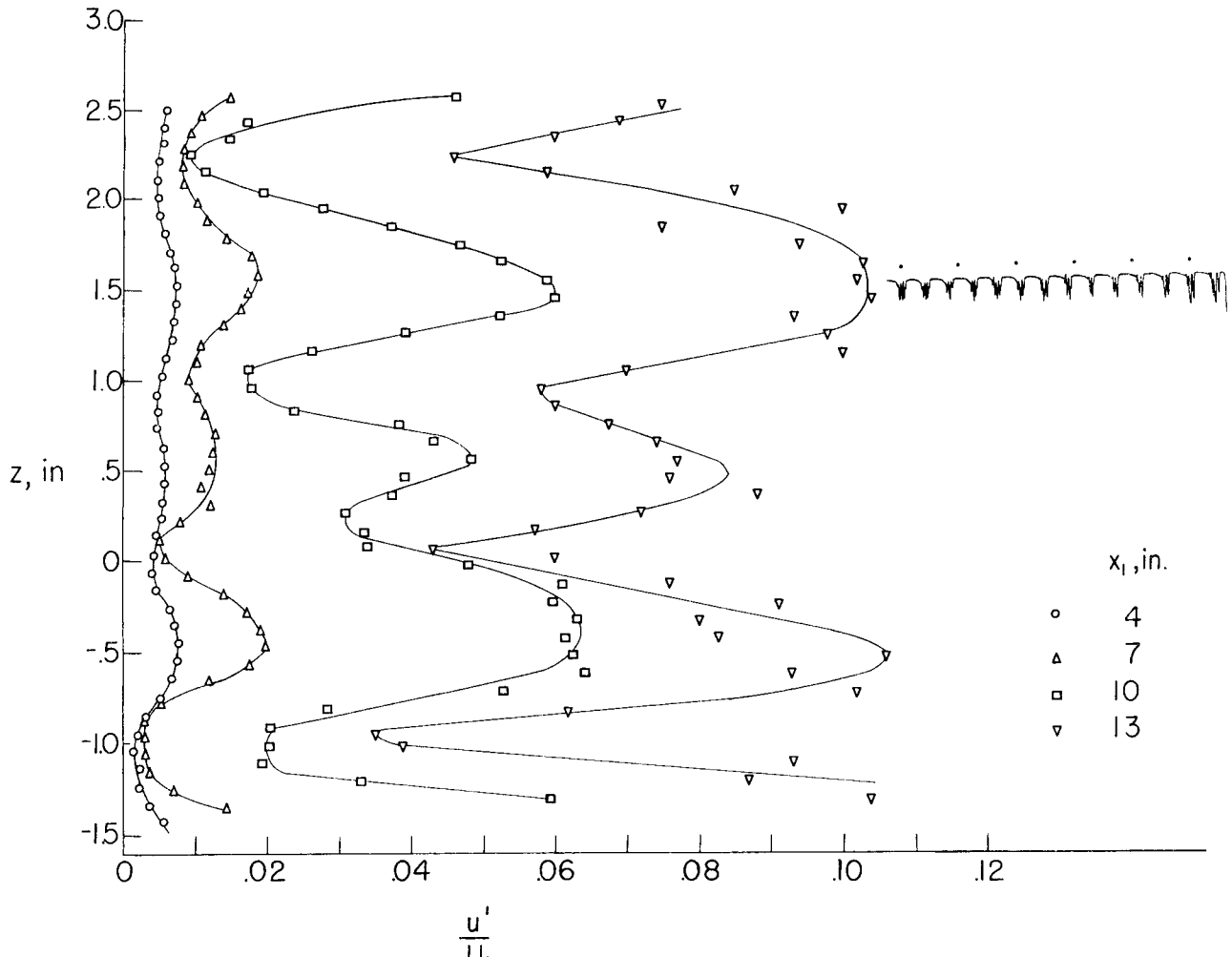


Figure 3. - Spanwise distribution of wave intensity at different distances downstream from vibrating ribbon. y = 0.046 inch; frequency, 145 cps. Oscillogram obtained at y = 0.12 inch illustrates characteristic breakdown of laminar flow occurring at peak. Time interval between dots, 1/60 second; time progression from right to left; increasing velocity toward timing signal.

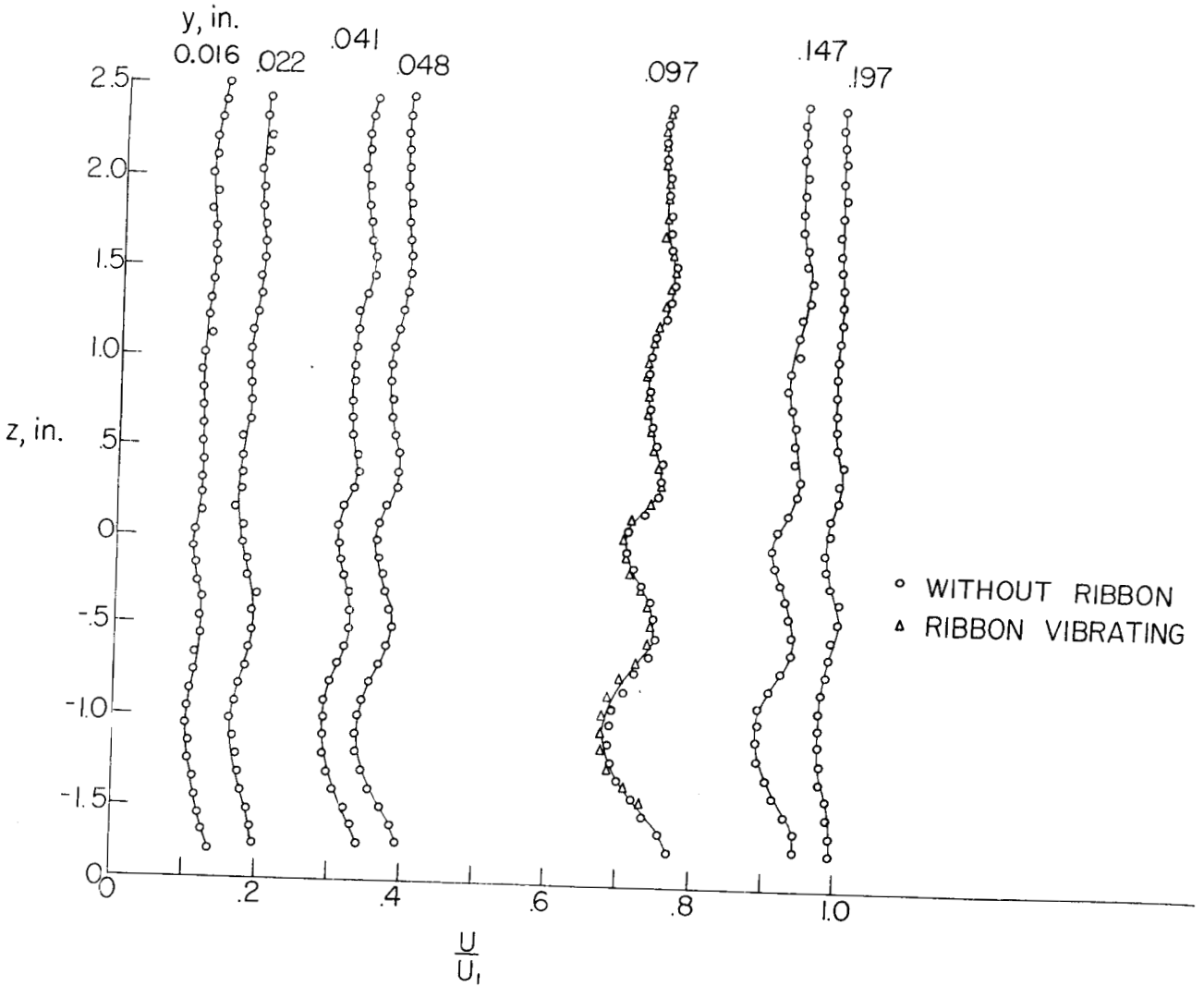


Figure 4. - Spanwise distribution of mean velocity for different positions across boundary layer at x = 3.5 feet.

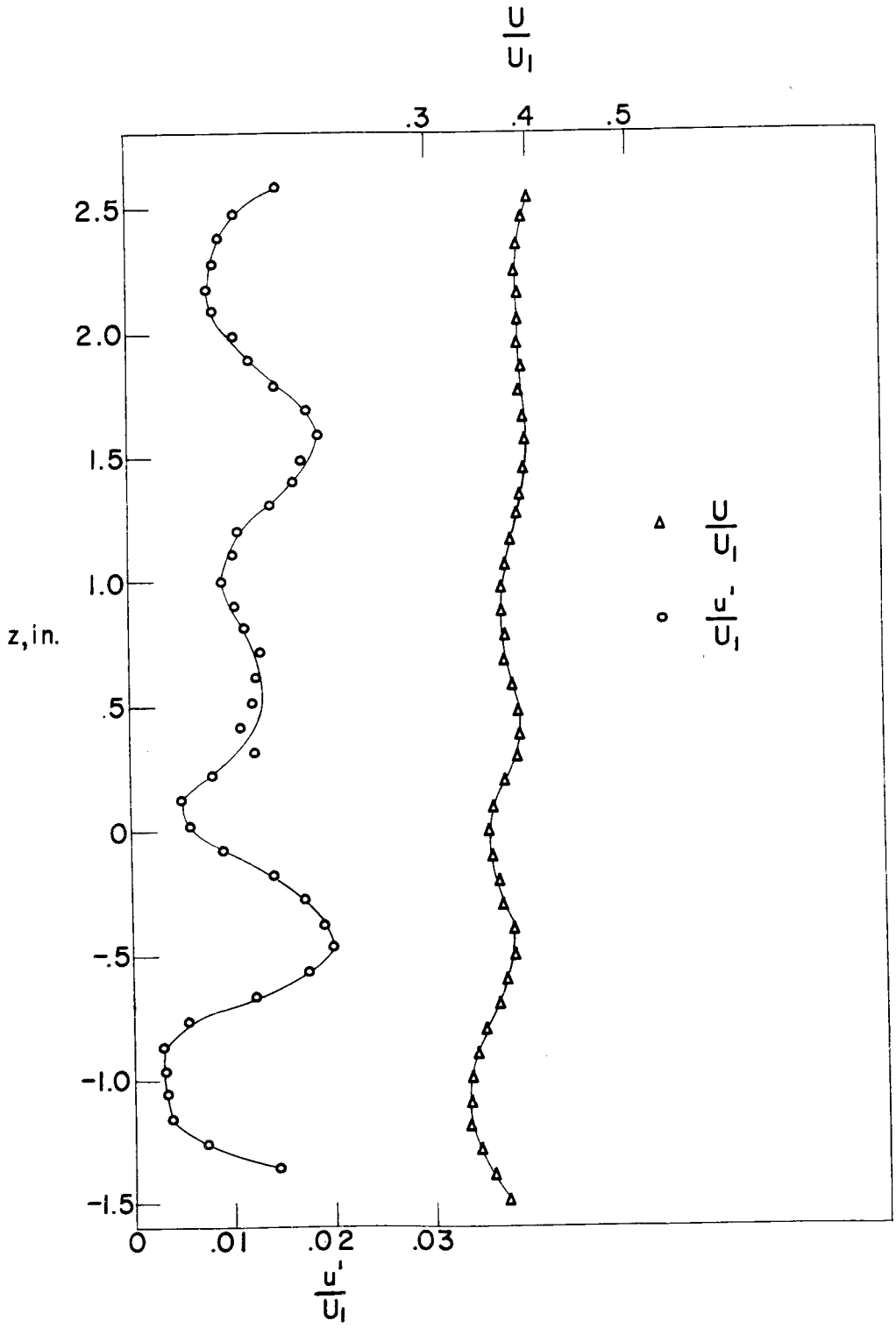


Figure 5. - Comparison of spanwise variations in mean velocity and wave intensity. $x_1$ = 7 inches; y = 0.046 inch; frequency, 145 cps.

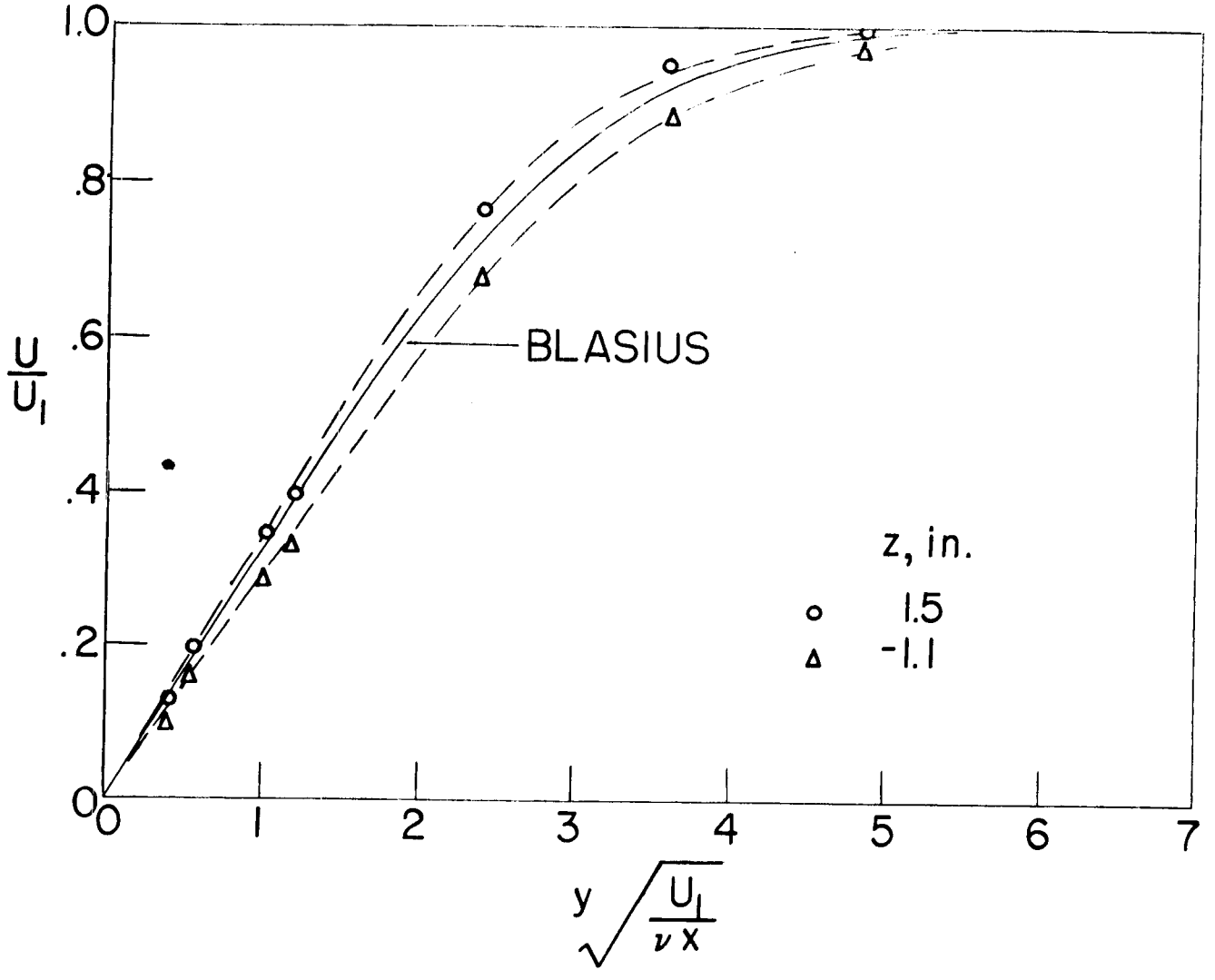


Figure 6. - Comparison of mean-velocity distributions at two spanwise positions with Blasius distribution. x = 3.5 feet.

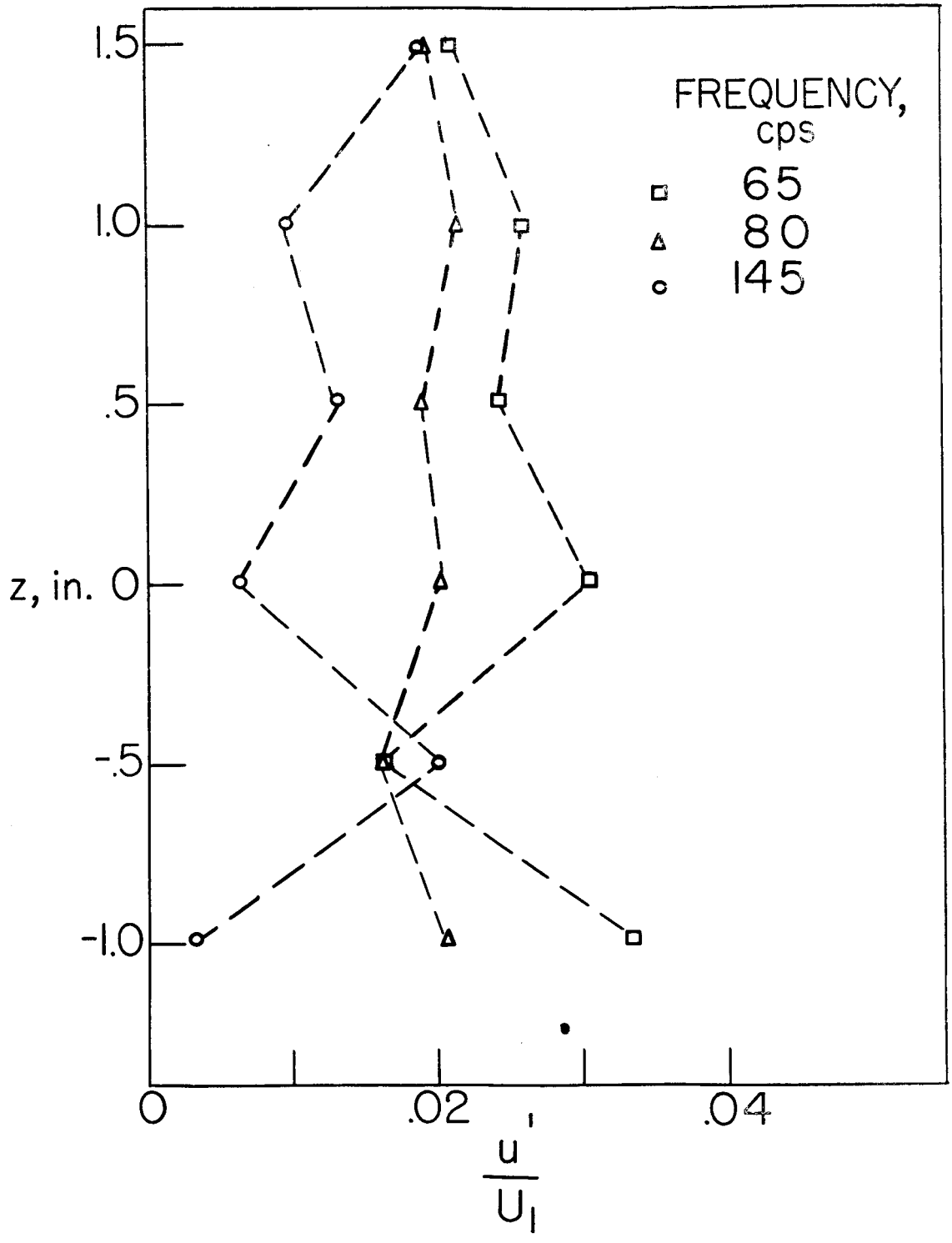


Figure 7. - Effect of frequency on spanwise variation in wave intensity. $x_1$ = 7 inches; y = 0.046 inch.

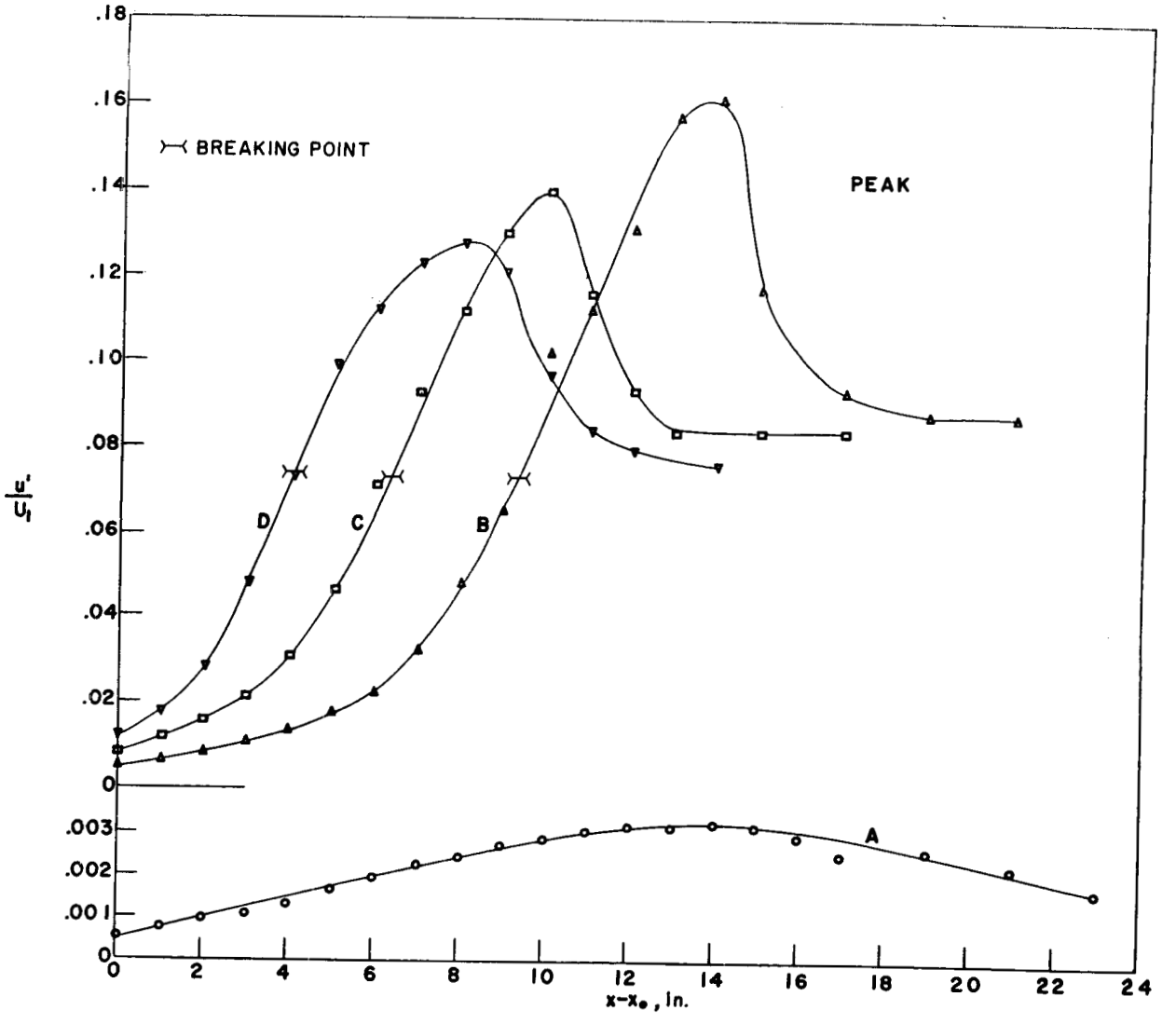


Figure 8. - Growth in wave intensity at peak for different input levels of vibrating ribbon. y = 0.046 inch; frequency, 145 cps.

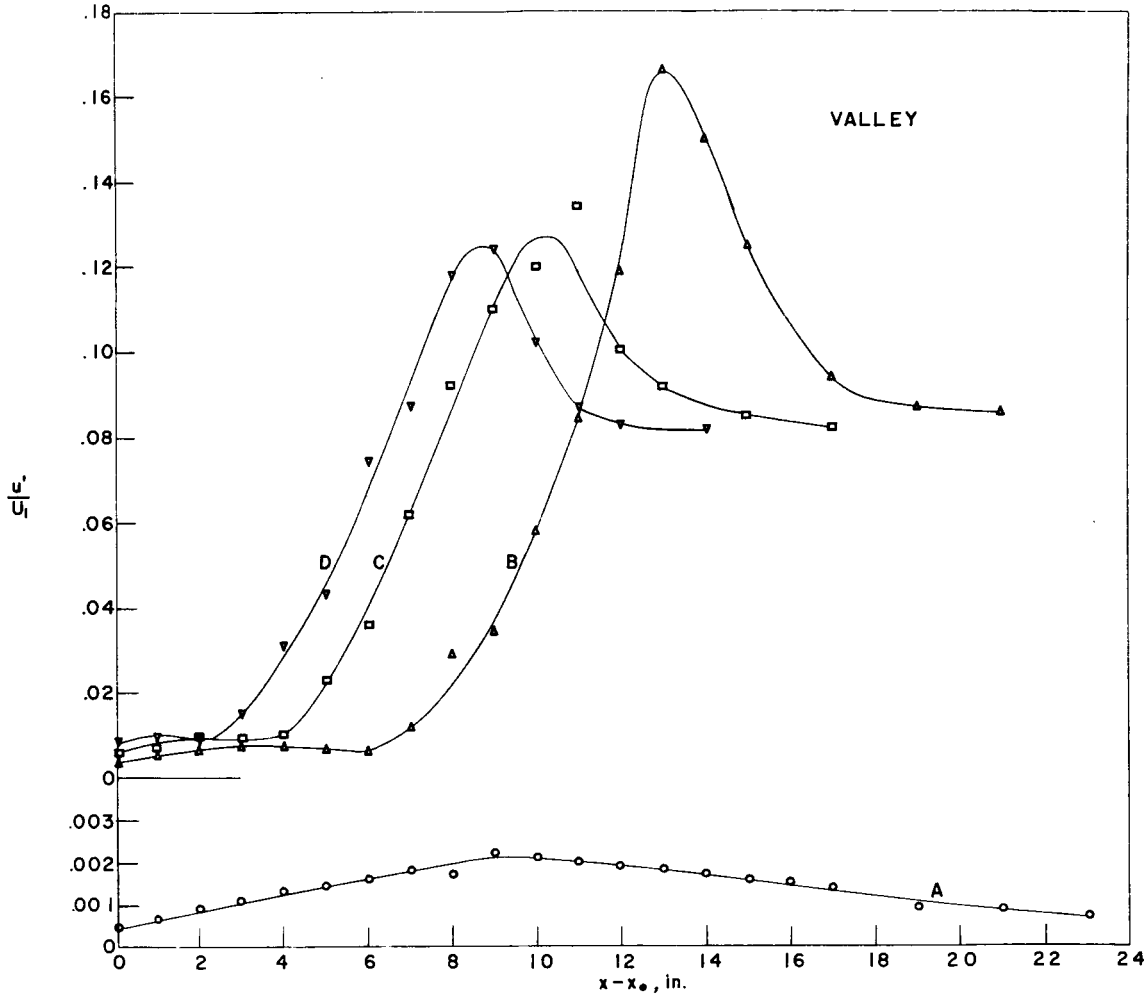


Figure 3. - Growth in wave intensity at valley for different input levels of vibrating ribbon. y = 0.046 inch; frequency, 145 cps.

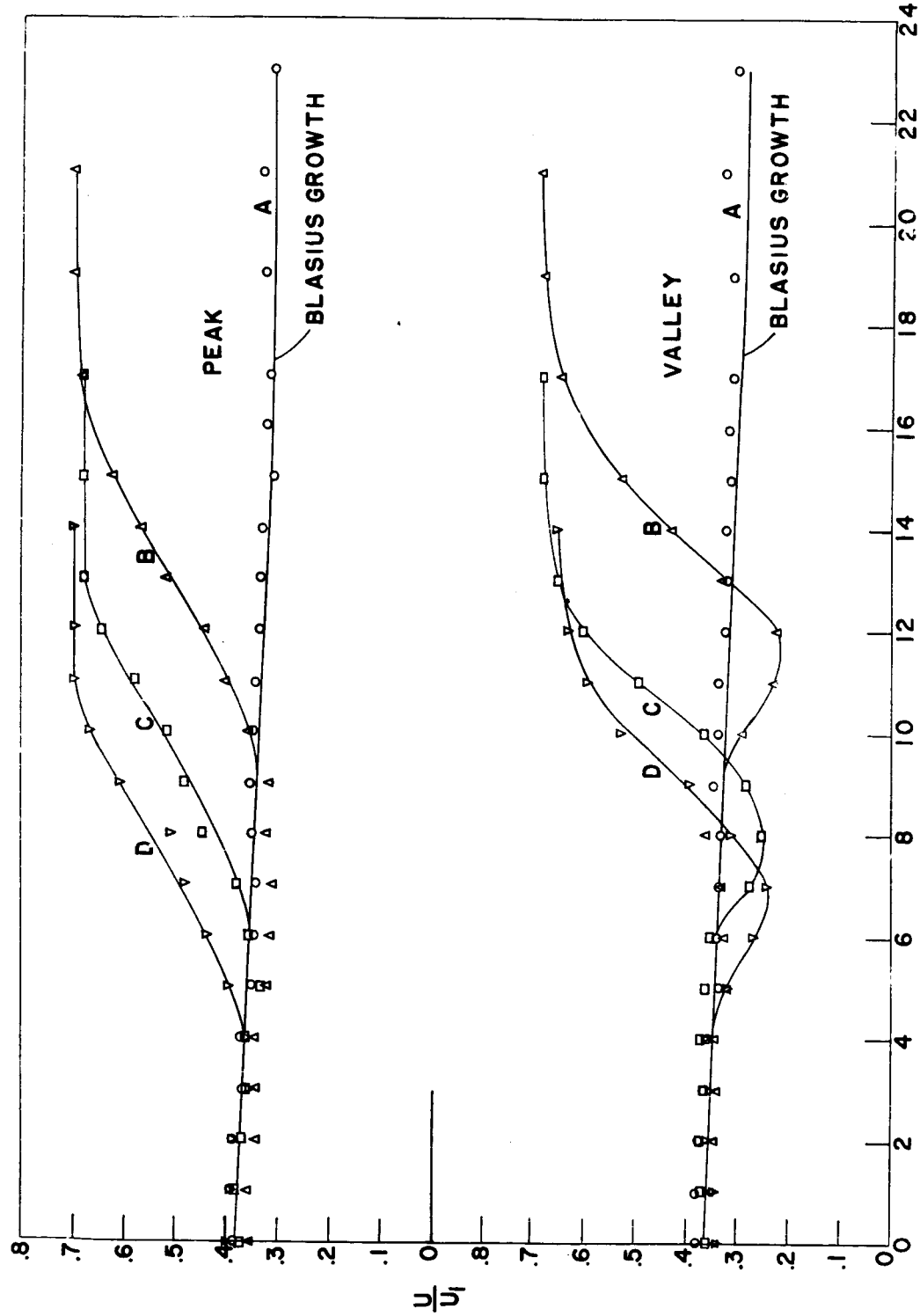


Figure 10. - Mean velocity at peak and valley associated with wave growth. y = 0.046 inch; frequency, 145 cps.

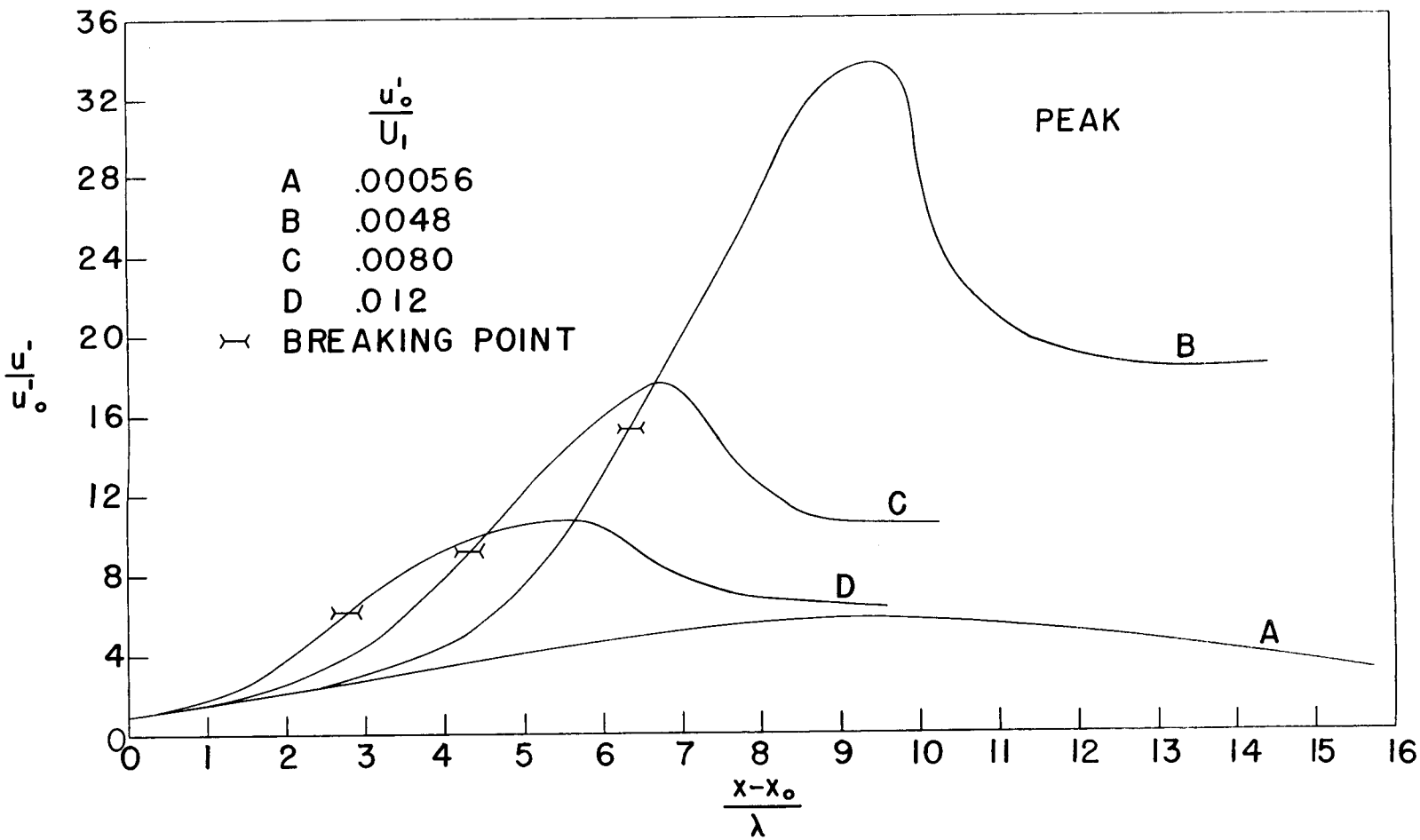


Figure 11. - Growth in wave intensity at peak shown nondimensionally relative to initial intensity and wave length of oscillation. Wave length, 1.46 inches; y = 0.046 inch; frequency, 145 cps.

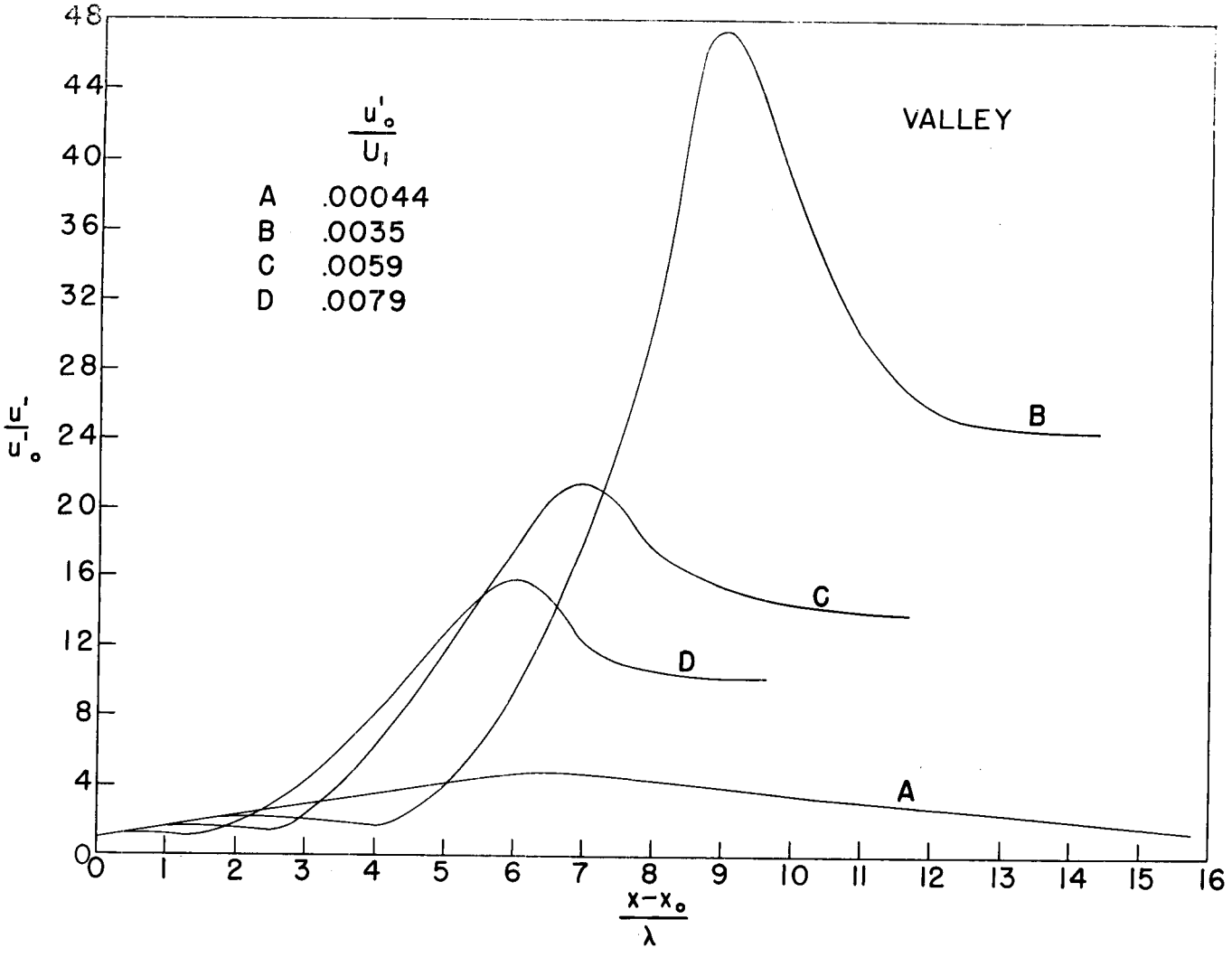


Figure 12. - Growth in wave intensity at valley shown nondimensionally relative to initial intensity and wave length of oscillation. Wave length, 1.46 inches; y = 0.046 inch; frequency, 145 cps.

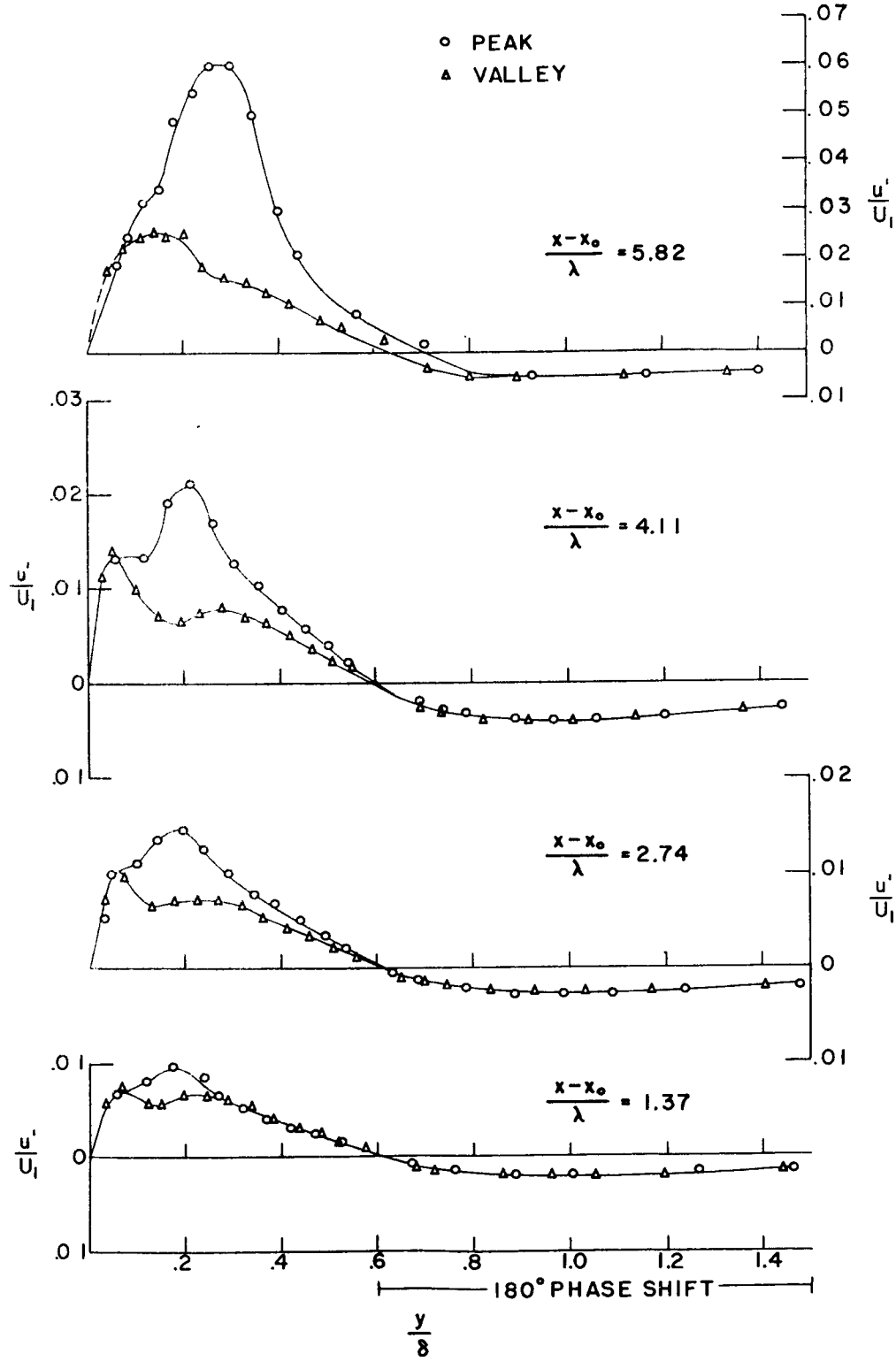


Figure 13. - Distribution of wave intensity for peak and valley at various stages of wave growth (curve B, figs. 11 and 12). Frequency, 145 cps.

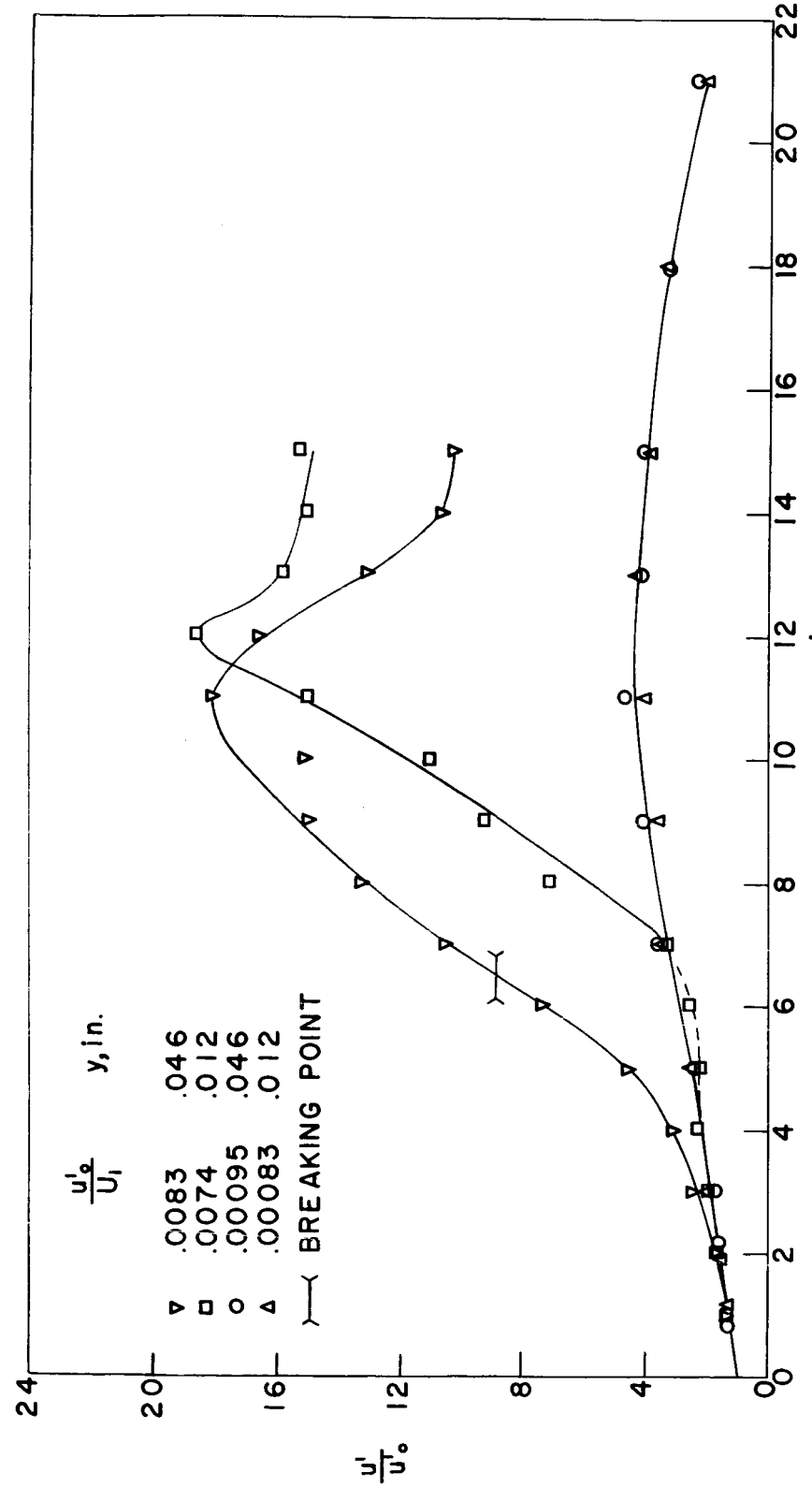


Figure 14. - Comparison of growth in wave intensity at y = 0.012 inch and y = 0.046 inch, at peak, for two input levels of vibrating ribbon. Frequency, 145 cps.

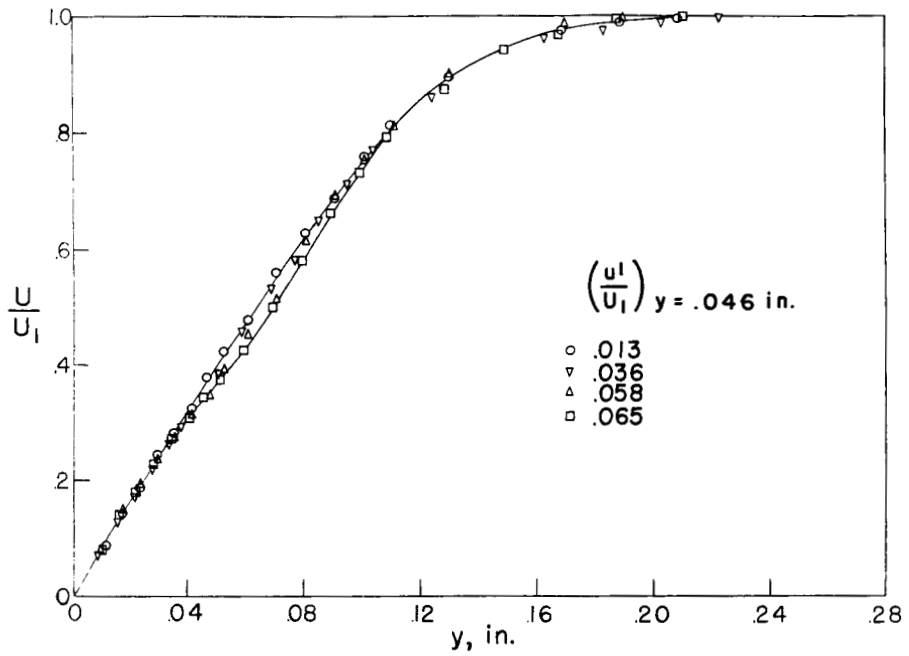


(a) IN REGION BEFORE BREAKDOWN.

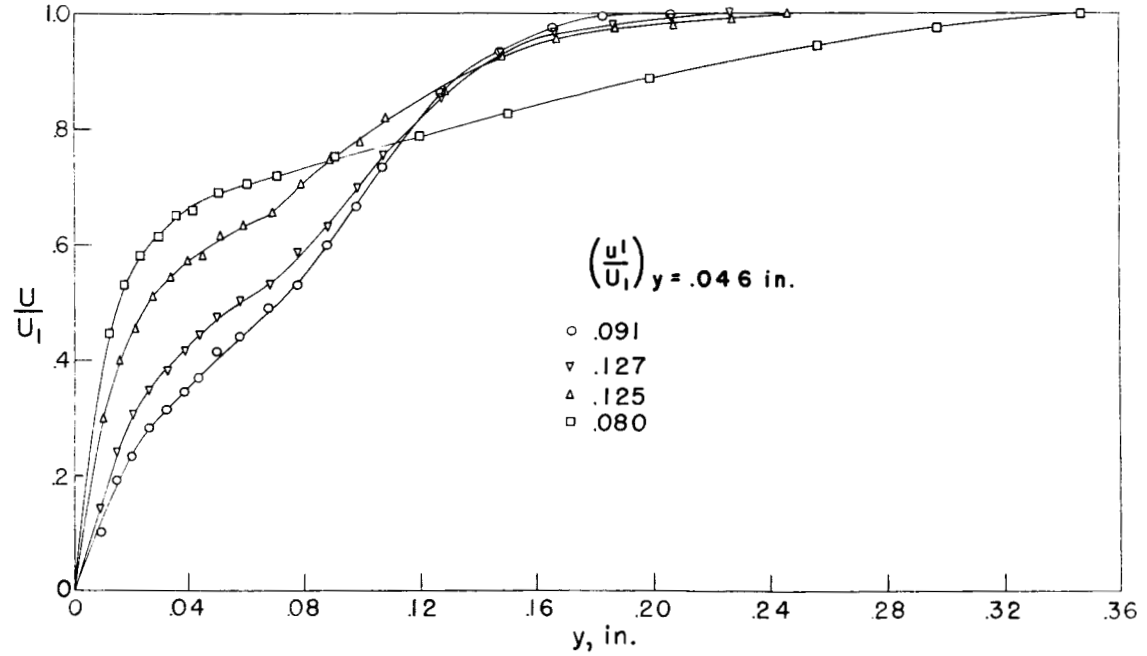


(b) IN REGION FROM BREAKDOWN TO FULLY DEVELOPED TURBULENT FLOW.

Figure 15. - Mean-velocity distributions at peak. $x_1$ = 10 inches; frequency, 145 cps.

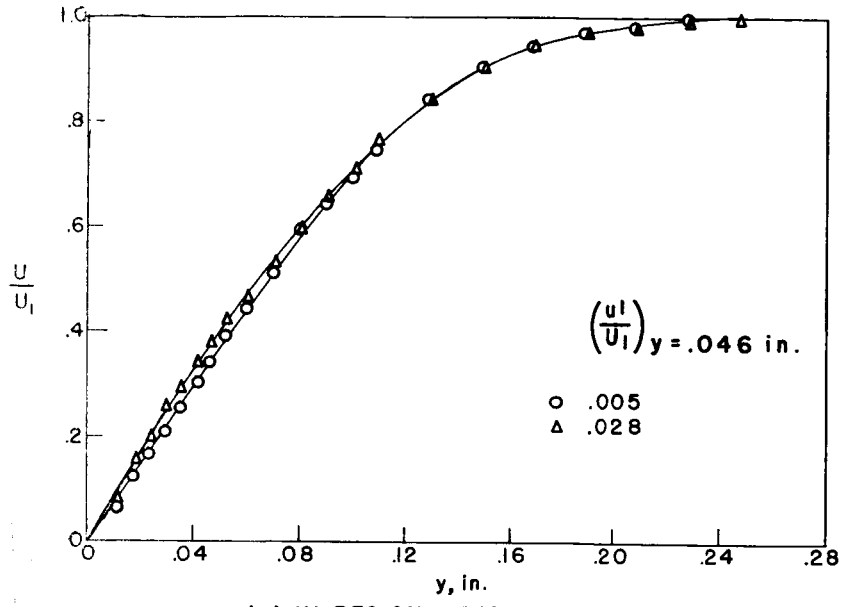


(a) IN REGION BEFORE BREAKOWN.

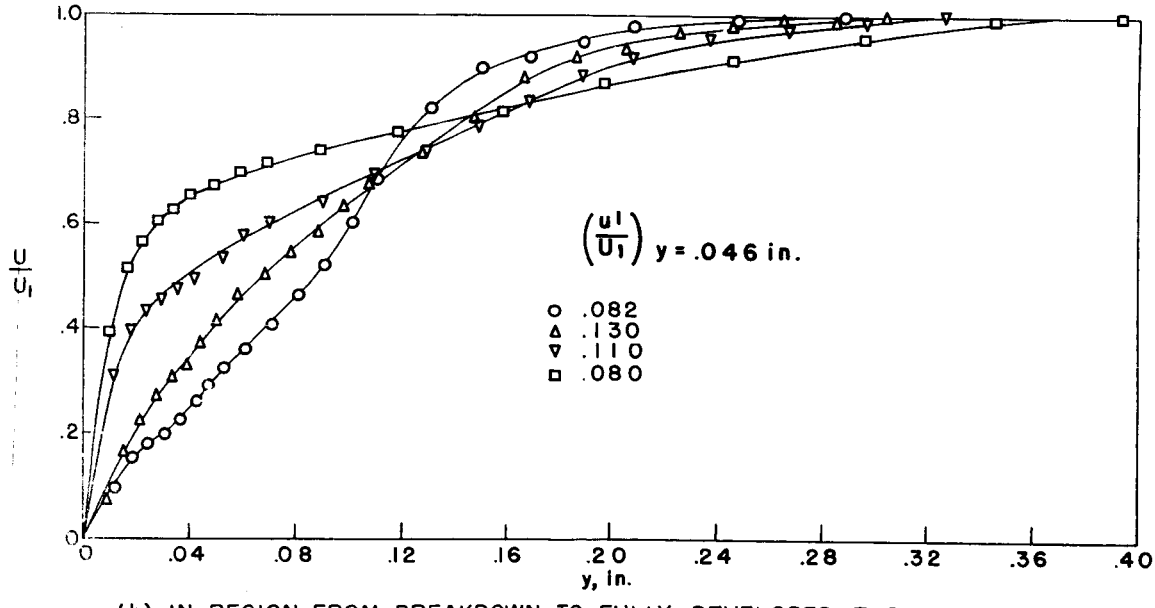


(b) IN REGION FROM BREAKDOWN TO FULLY DEVELOPED TURBULENT FLOW.

Figure 16. - Mean-velocity distributions at valley. $x_1$ = 10 inches; frequency, 145 cps.

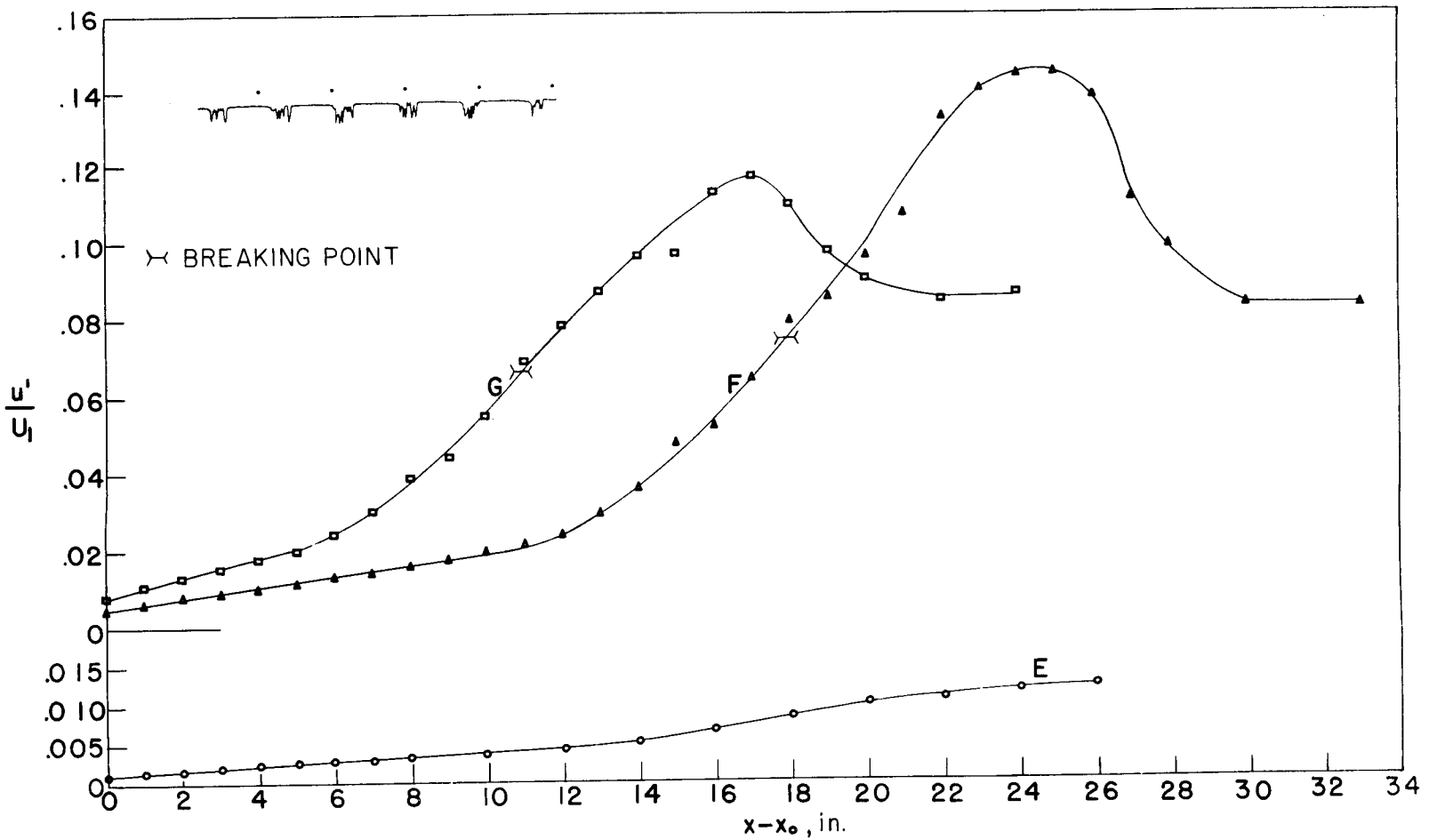


Figure 17. - Growth in wave intensity at peak for different input levels of vibrating ribbon. y = 0.046 inch; frequency, 70 cps. Oscillogram obtained at y = 0.12 inch illustrates characteristic breakdown of laminar flow. Time interval between dots, 1/60 second; time progression from right to left; increasing velocity toward timing signal.

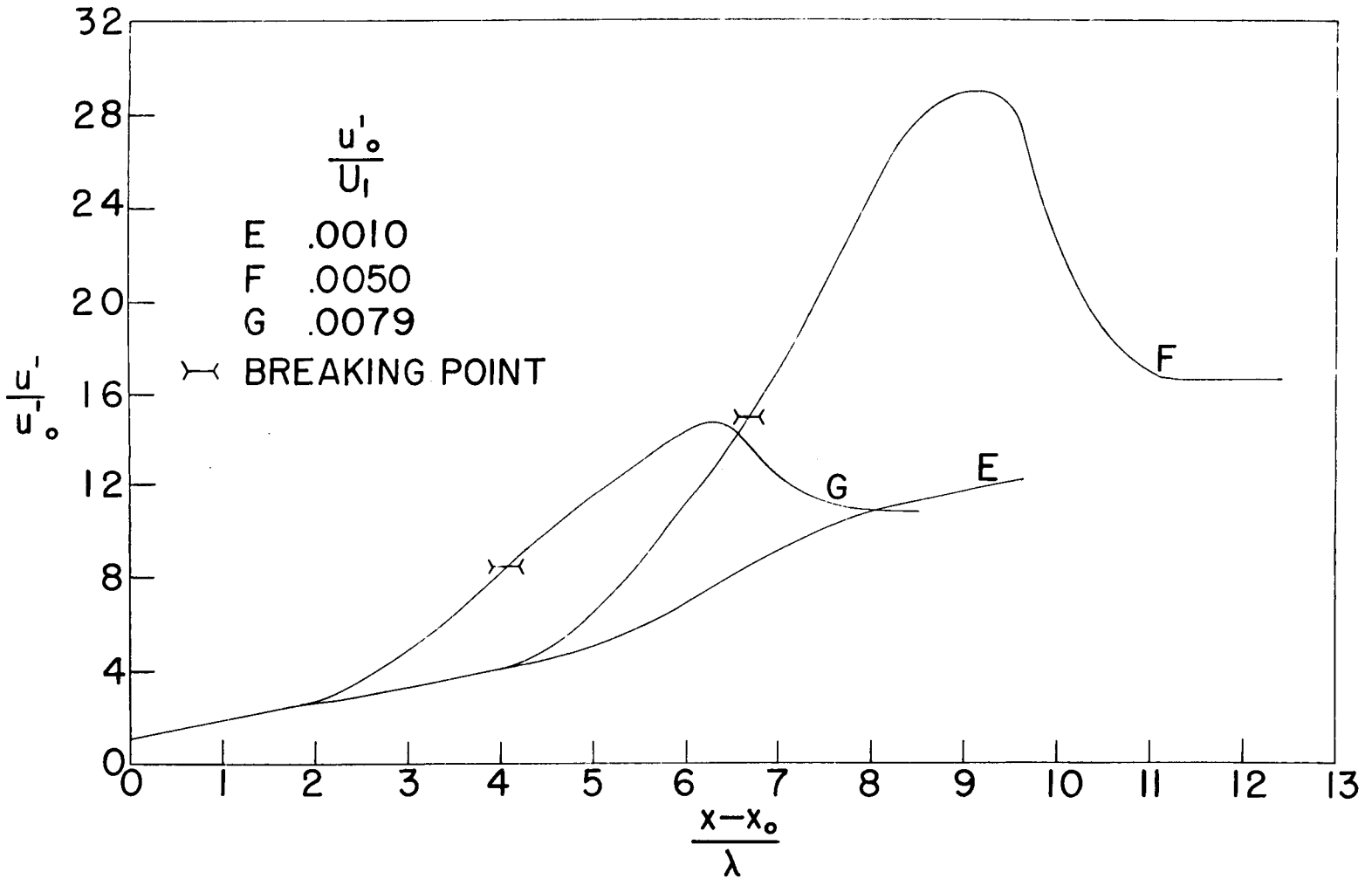


Figure 18. - Growth in wave intensity at peak shown nondimensionally relative to initial intensity and wave length of oscillation. Wave length, 2.7 inches; y = 0.046 inch; frequency, 70 cps.

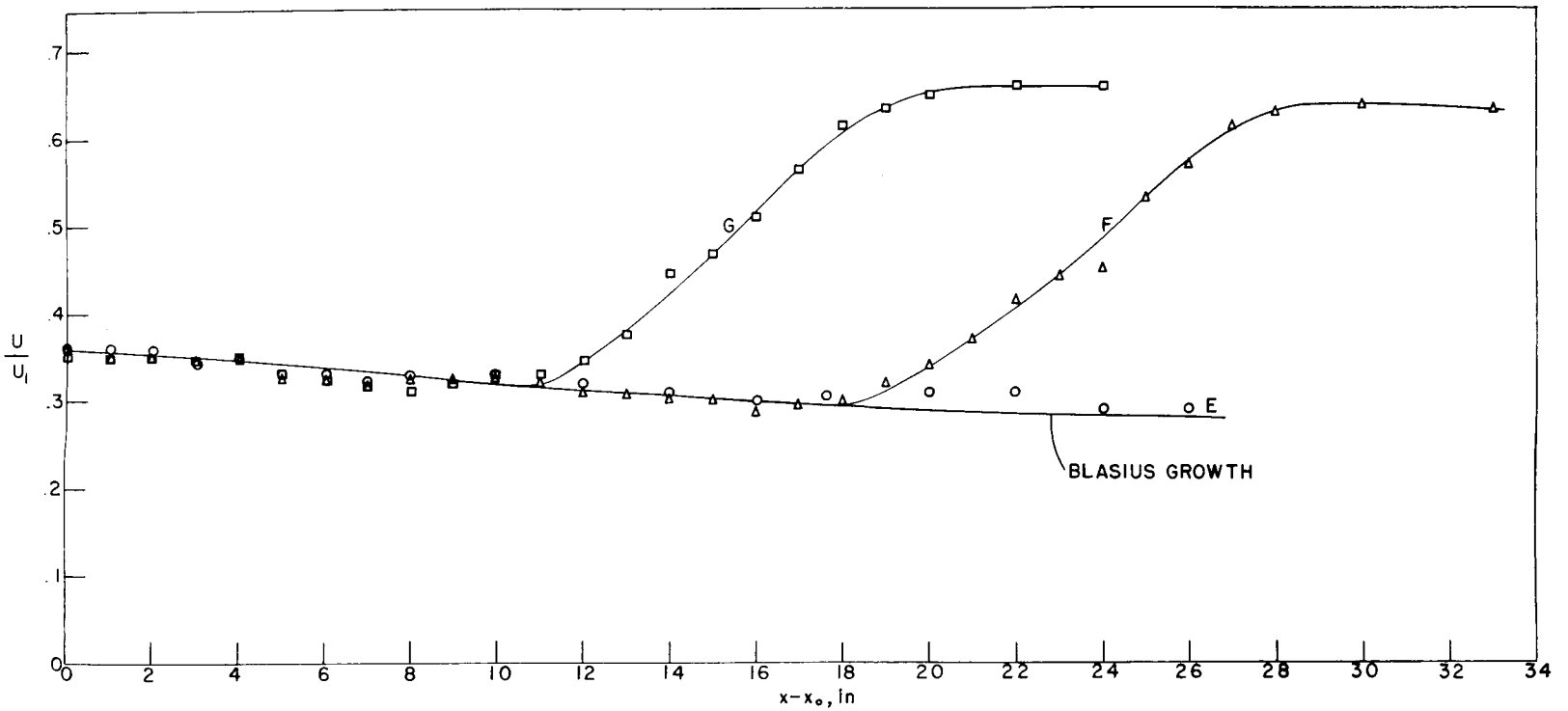


Figure 19. - Mean velocity at peak associated with wave growth. y = 0.046 inch; frequency, 70 cps.

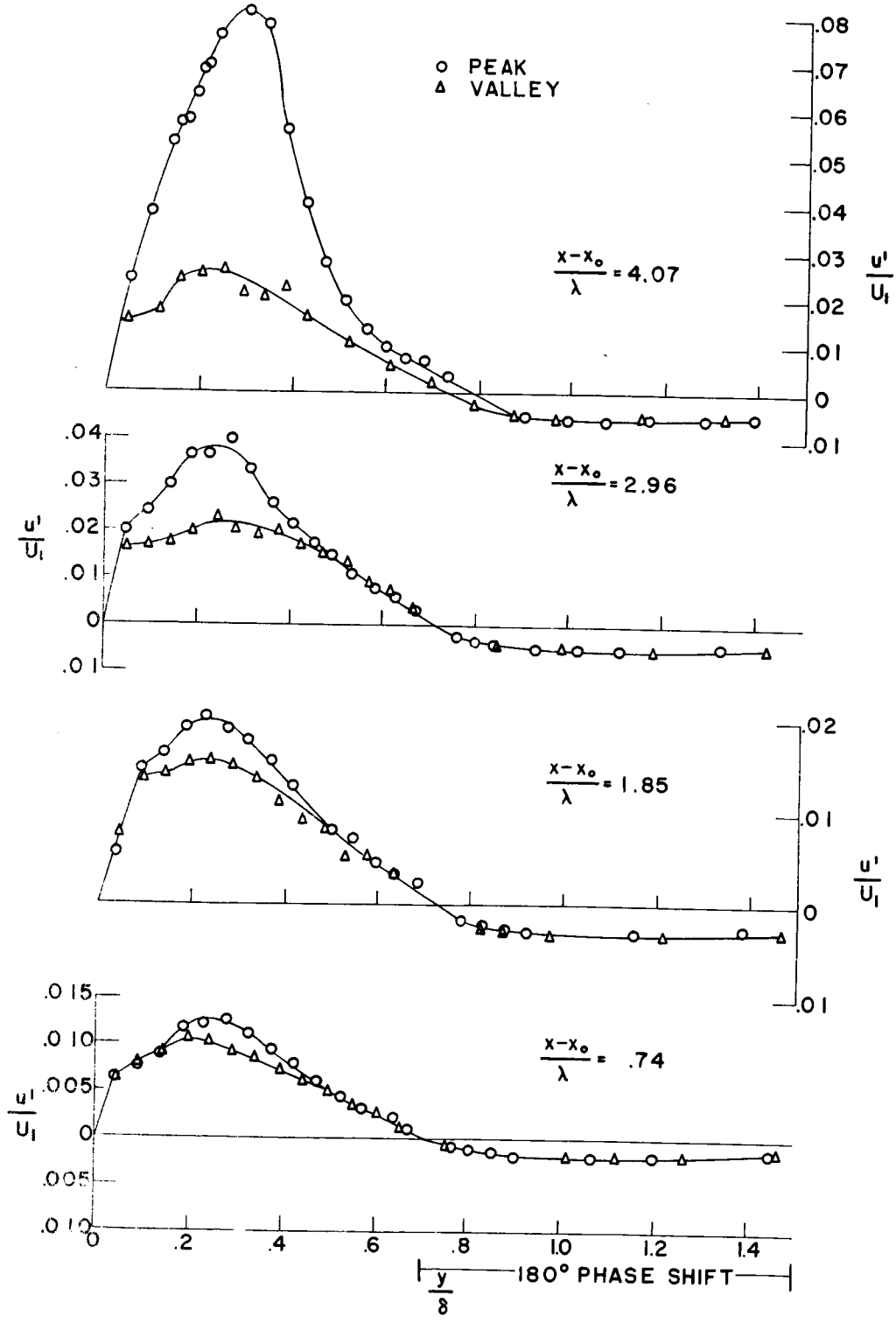


Figure 20. - Distribution of wave intensity for peak and valley at various stages of wave growth (curve G, figs. 18 and 19). Frequency, 70 cps.

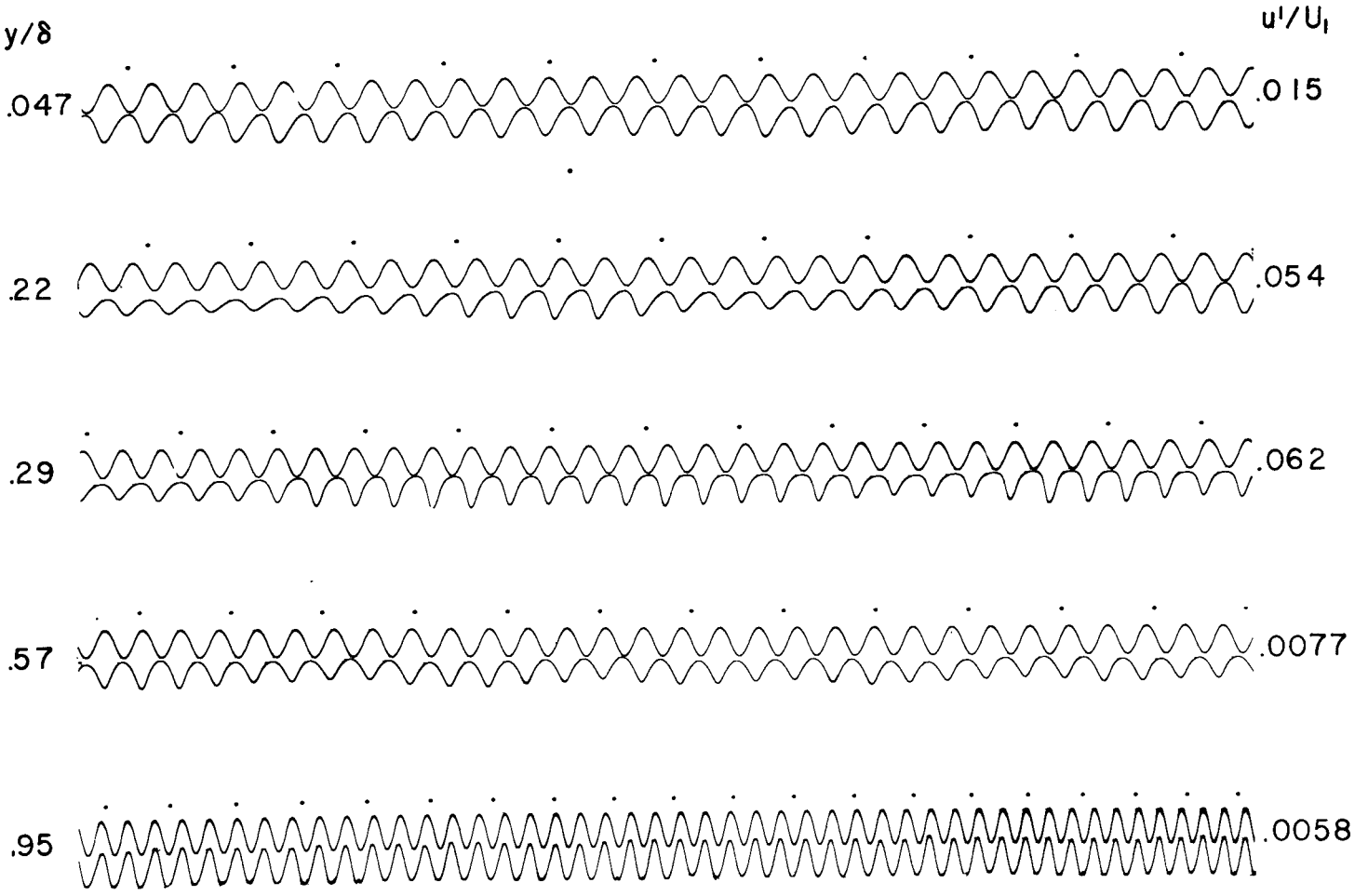


Figure 21. - Oscillograms of u-fluctuation at peak. Frequency, 145 cps; top trace in each oscillogram is reference signal. Time interval between dots, 1/60 second; time progression from right to left; increasing velocity toward timing signal.


Figure 22. - Oscillograms of u-fluctuation at valley. Frequency, 145 cps; top trace in each oscillogram is reference signal. Time interval between dots, 1/60 second; time progression from right to left; increasing velocity toward timing signal.

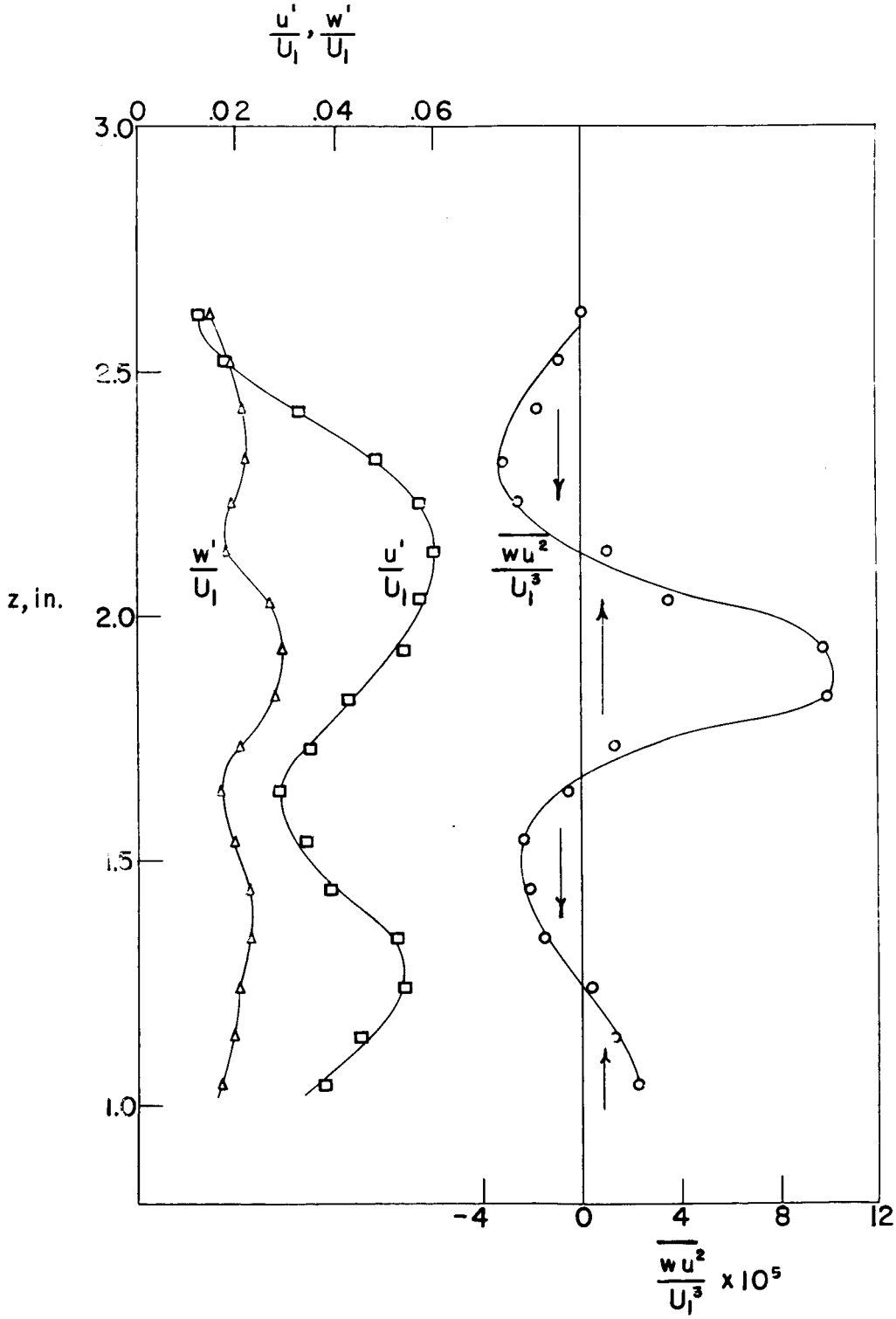


Figure 23. - Spanwise energy transfer and spanwise distributions of u' and w'. $x_1$ = 7 inches; y = 0.046 inch; frequency, 145 cps.

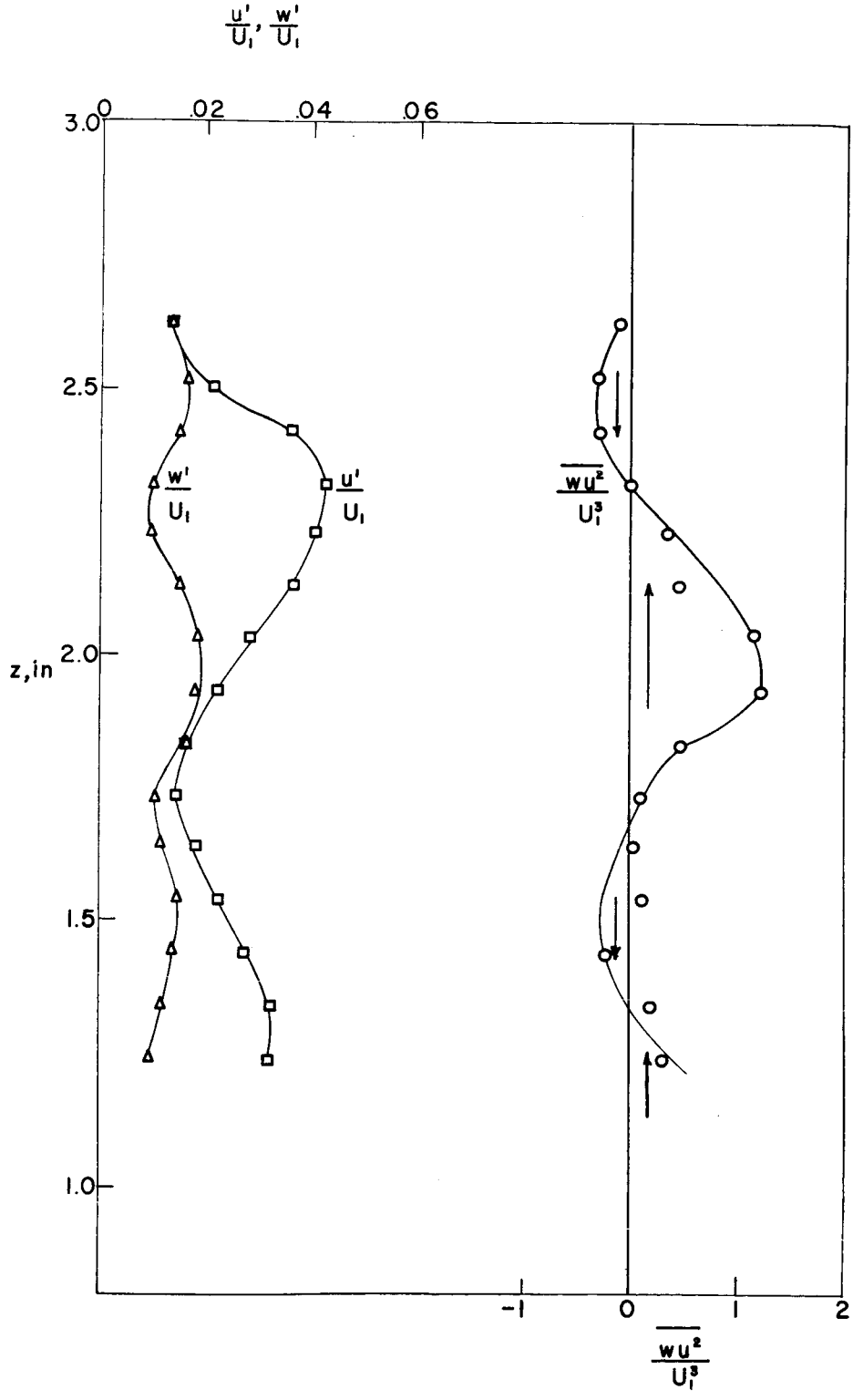


Figure 24. - Spanwise energy transfer and spanwise distributions of u' and w'. $x_1$ = 7 inches; y = 0.046 inch; frequency, 145 cps.

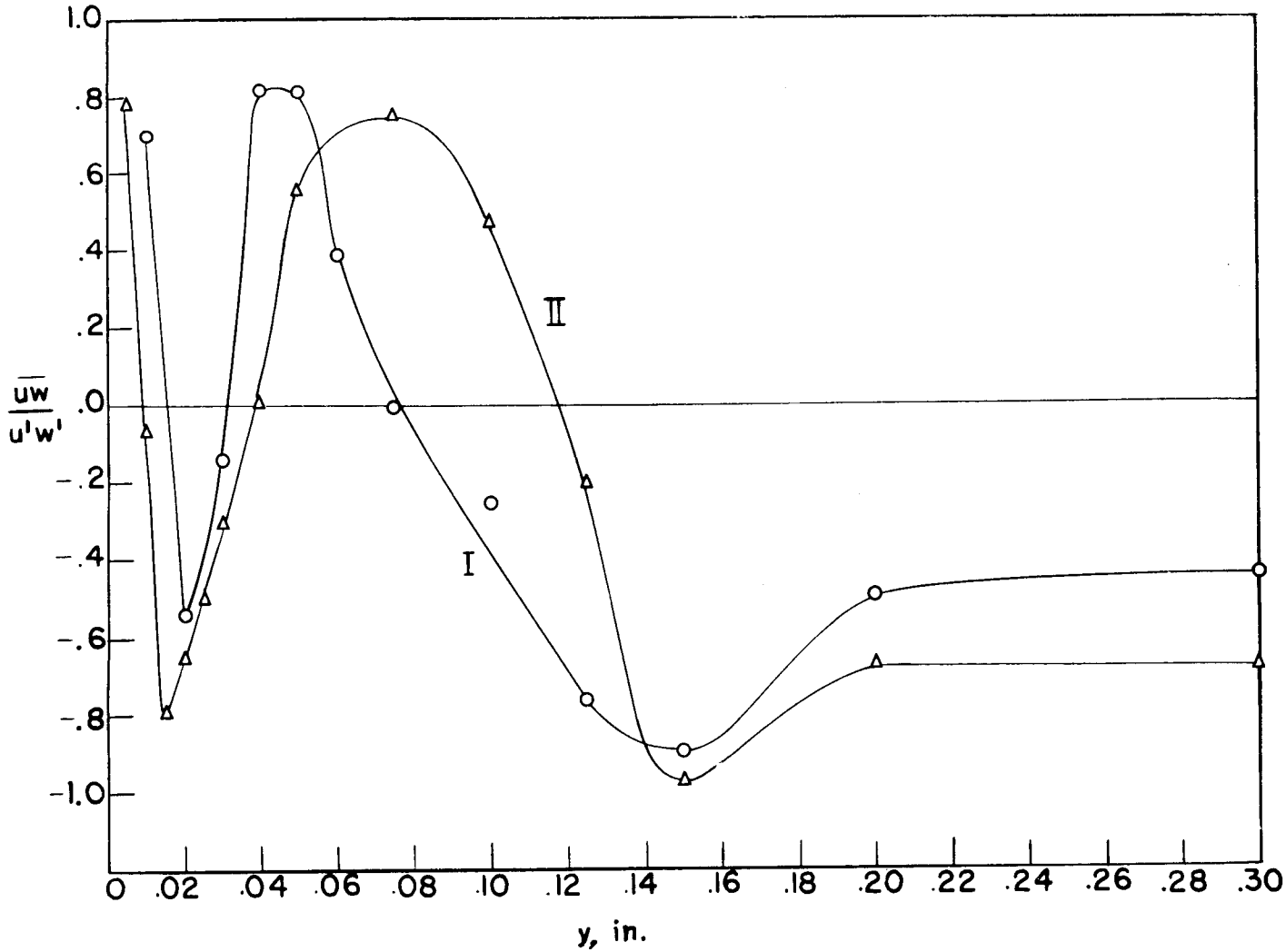


Figure 25. - Correlation between u- and w-fluctuations. z = 2.1 inches; $x_1$ = 7 inches; frequency, 145 cps.

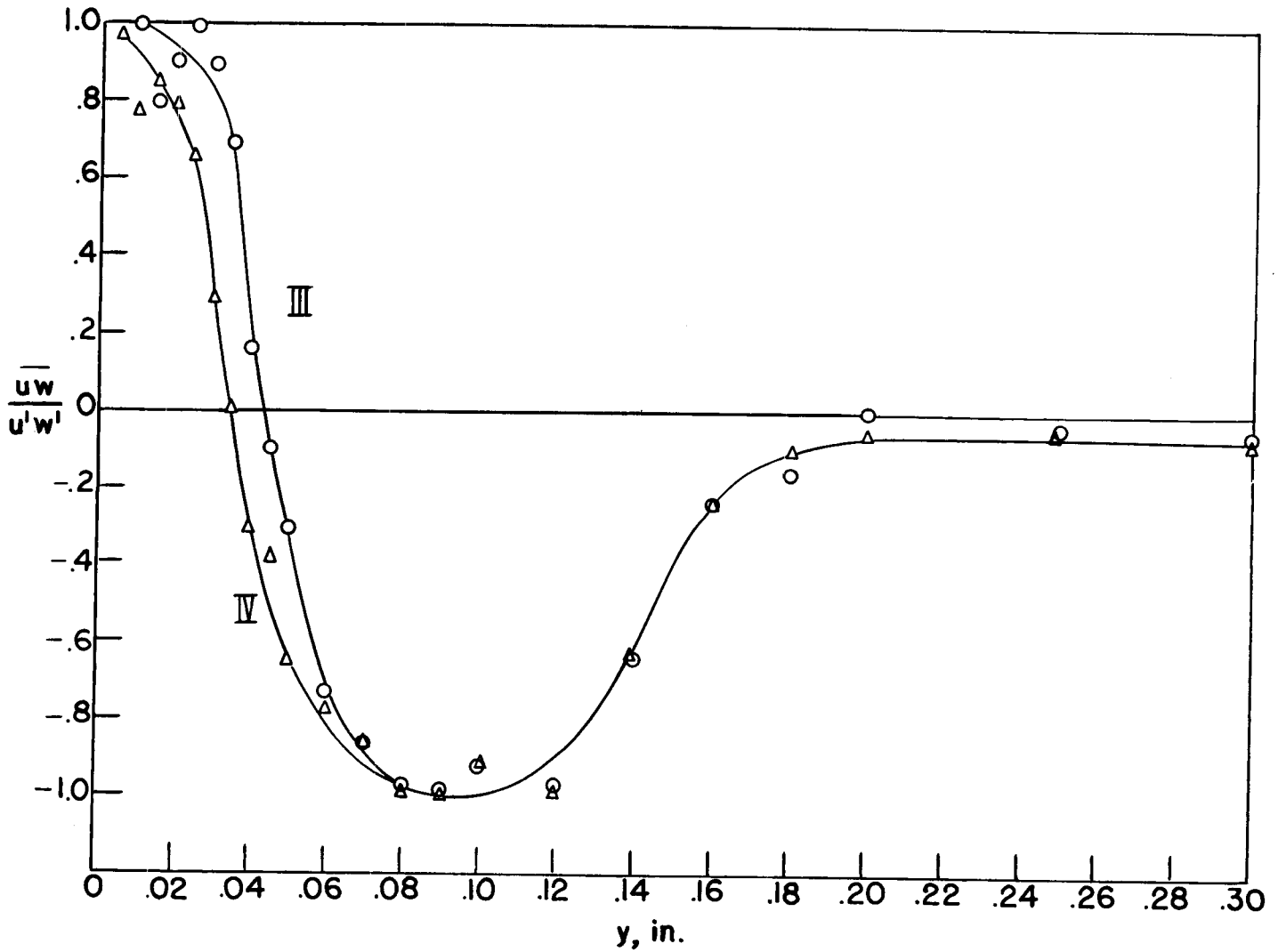


Figure 26. - Correlation between u- and w-fluctuations. z = 2.5 inches; $x_1$ = 7 inches; frequency, 145 cps.

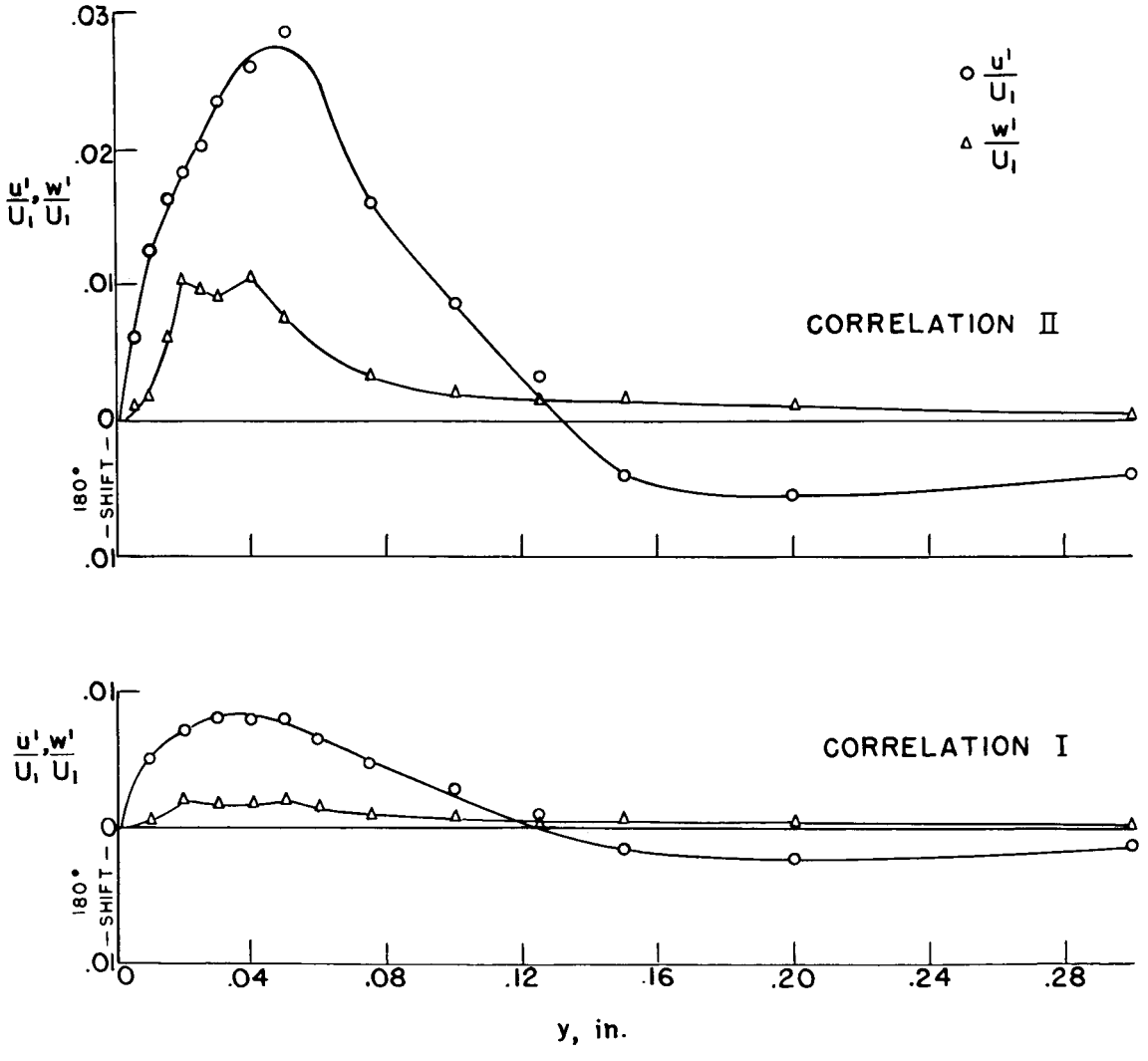


Figure 27. - Distributions of u' and w'. z = 2.1 inches; $x_1$ = 7 inches; frequency, 145 cps.

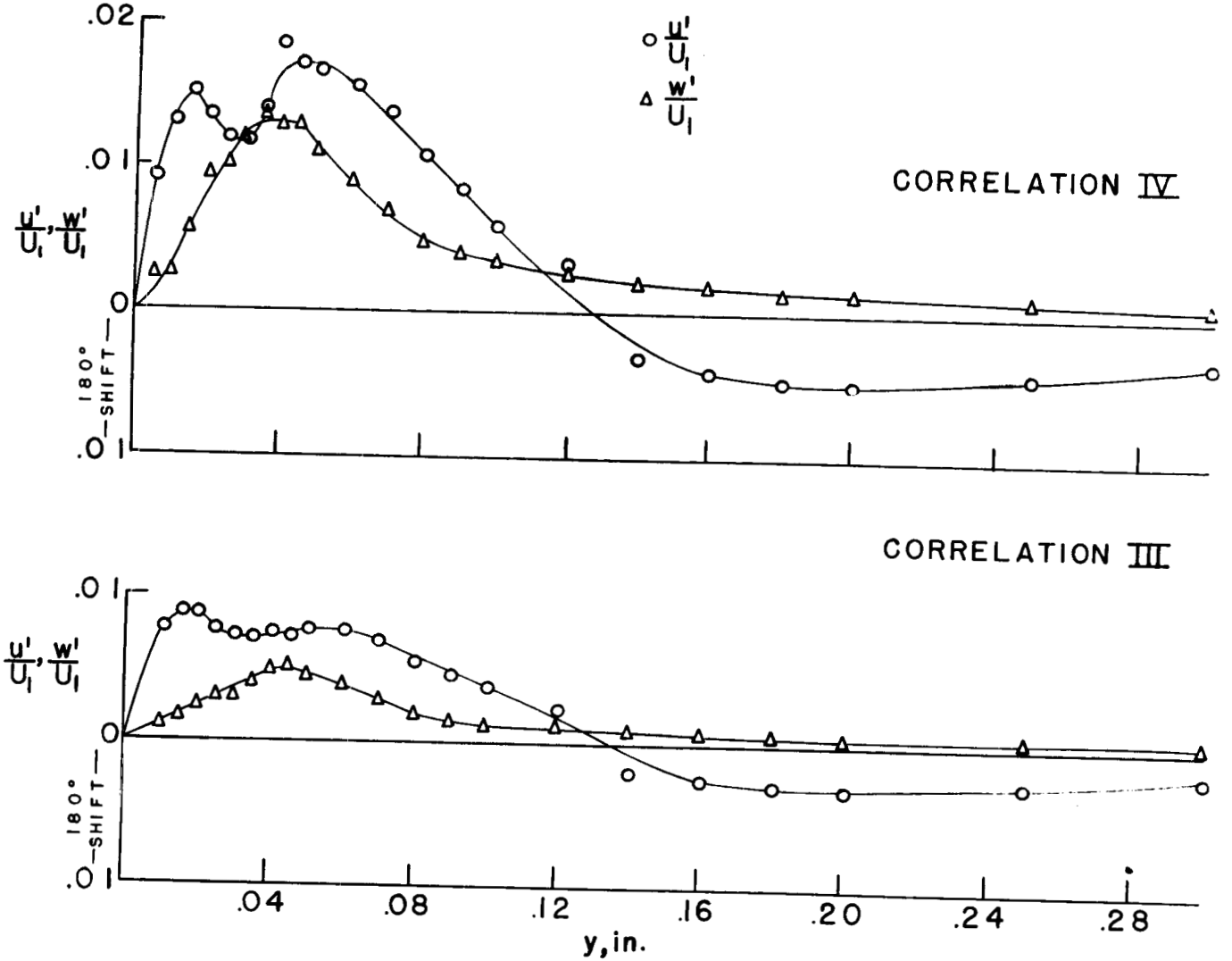


Figure 28. - Distributions of u' and w'. z = 2.5 inches; $x_1$ = 7 inches; frequency, 145 cps.


Figure 29. - Oscillograms of simultaneous u- and w-fluctuations. z = 2.1 inches; $x_1$ = 7 inches; frequency, 145 cps. Top trace in each oscillogram is w-fluctuation. Time interval between dots, 1/60 second; time progression from right to left; increasing velocity toward timing signal.


Figure 30. - Oscillograms of simultaneous u- and w-fluctuations. z = 2.5 inches; $x_1$ = 7 inches; frequency, 145 cps. Top trace in each oscillogram is w-fluctuation. Time interval between dots, 1/60 second; time progression from right to left; increasing velocity toward timing signal.

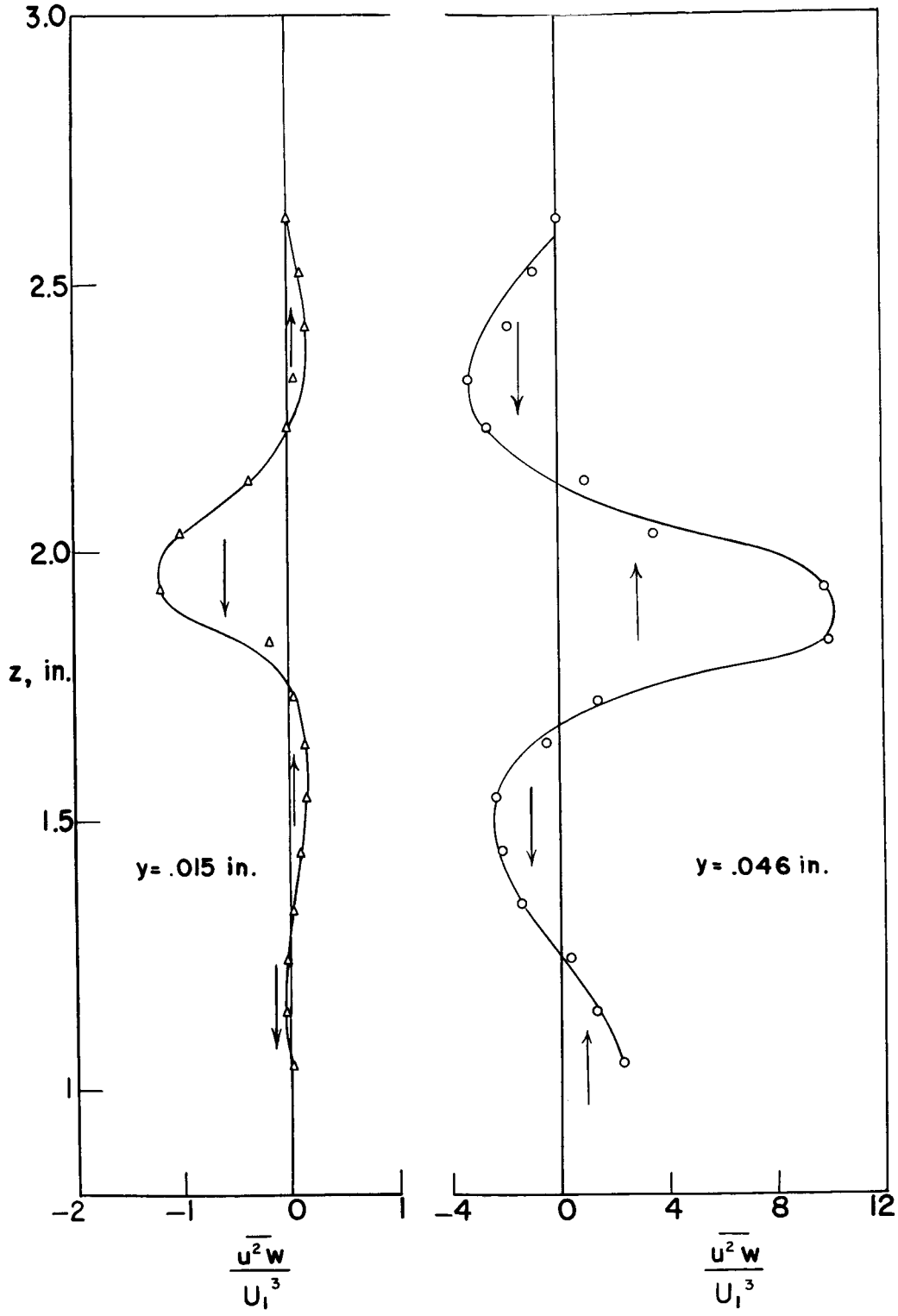


Figure 31. - Comparison of spanwise energy transfer at y = 0.015 inch and y = 0.046 inch. $x_1$ = 7 inches; frequency, 145 cps.

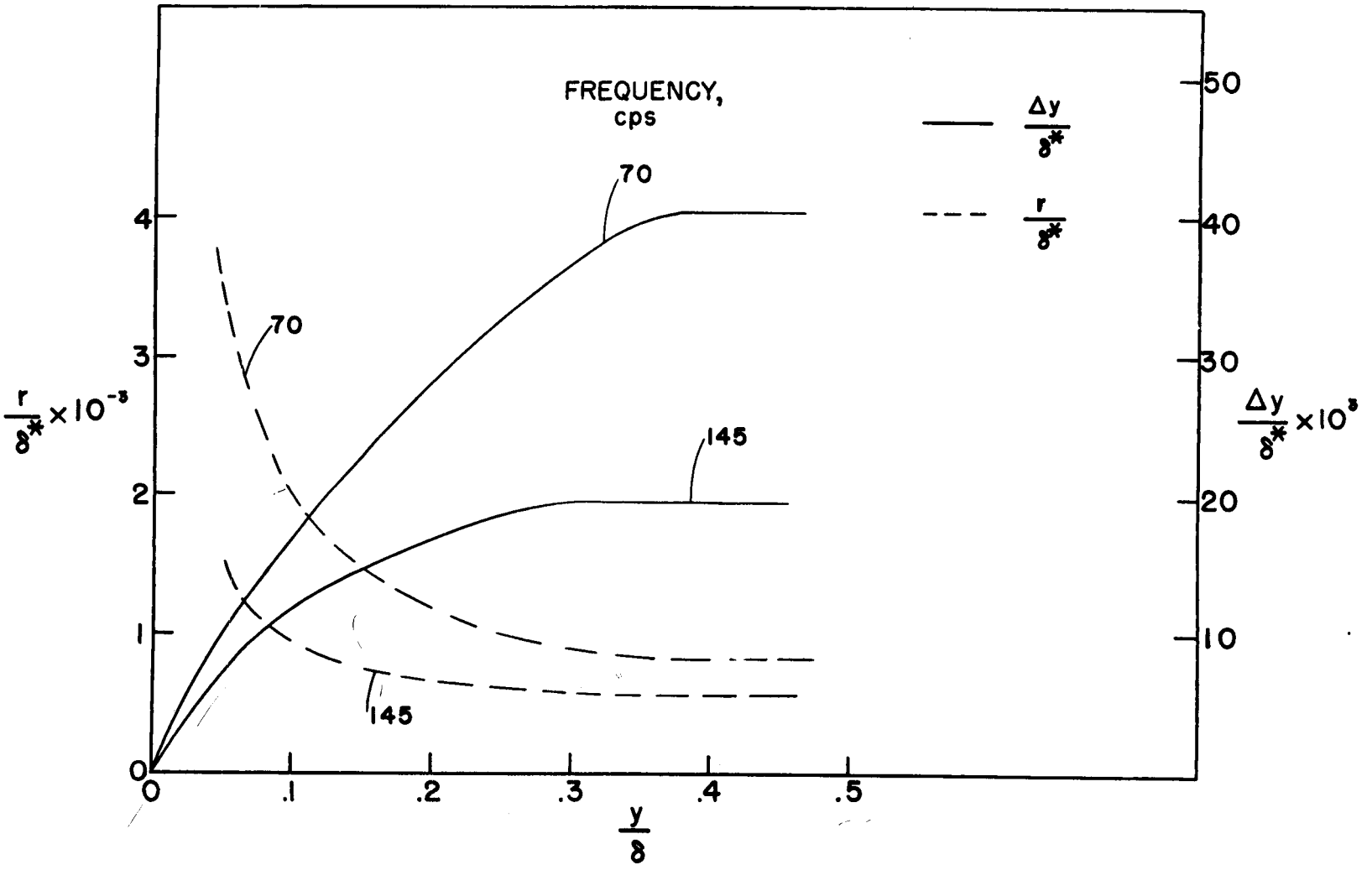


Figure 32. - Streamline radius of curvature and streamline displacement at peak pertaining to point of departure from linear-theory amplification rate.

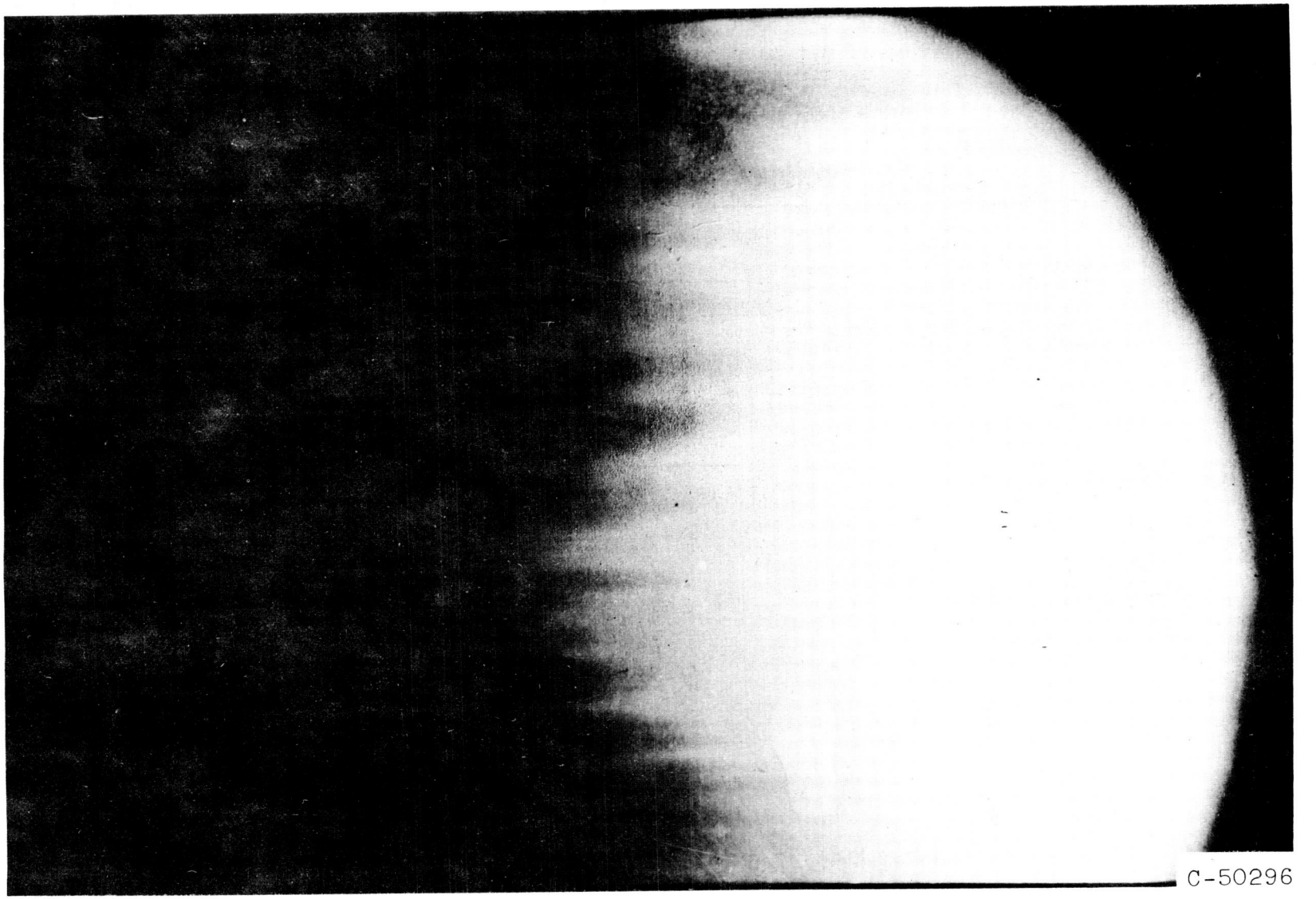


Figure 33. - Transition pattern as shown by China-clay technique.

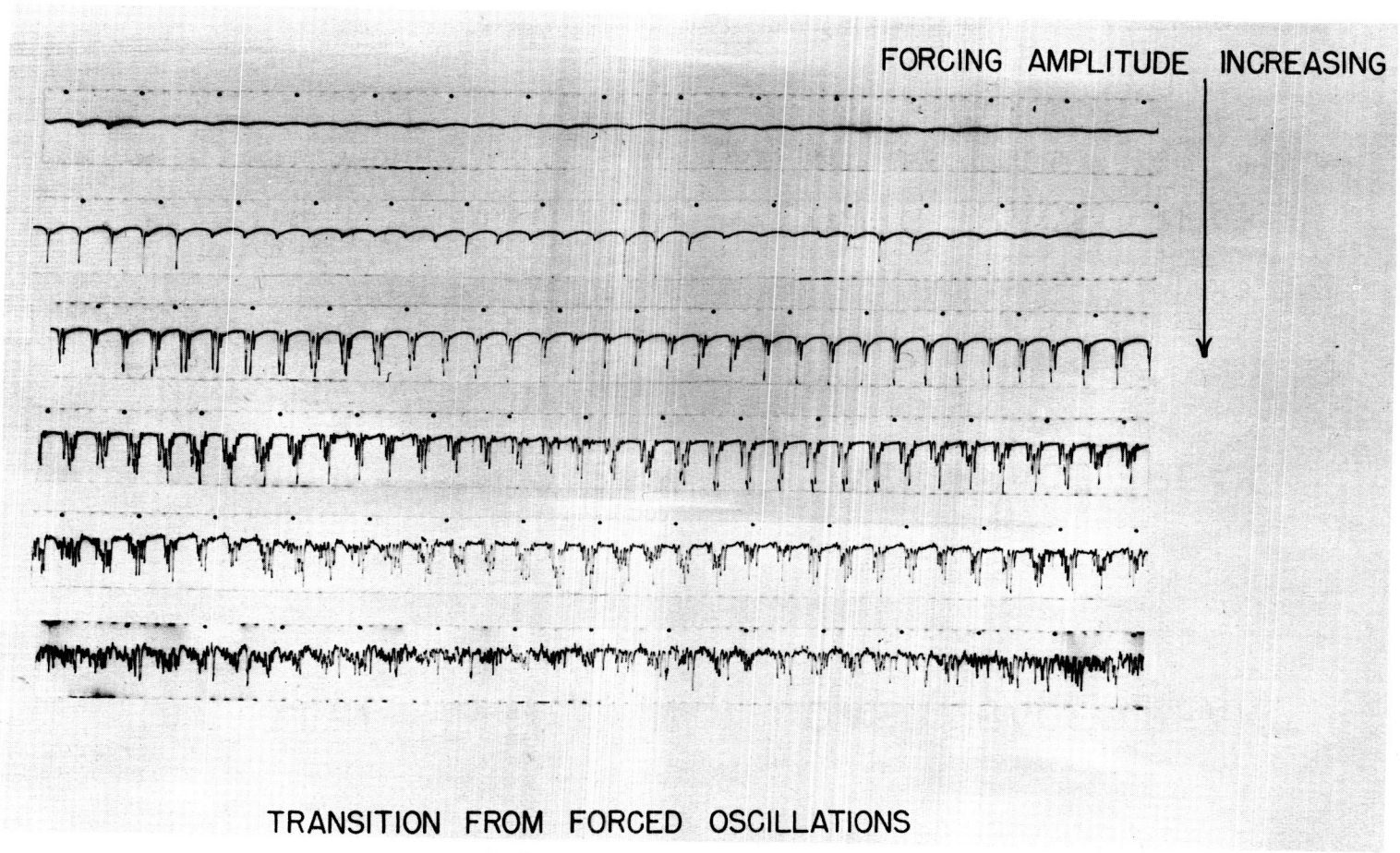


Figure 34. - Oscillograms illustrating progression from initial breakdown to fully turbulent flow at peak. y = 0.12 inch; frequency, 145 cps. Time interval between dots, 1/60 second; time progression from right to left; increasing velocity toward timing signal.

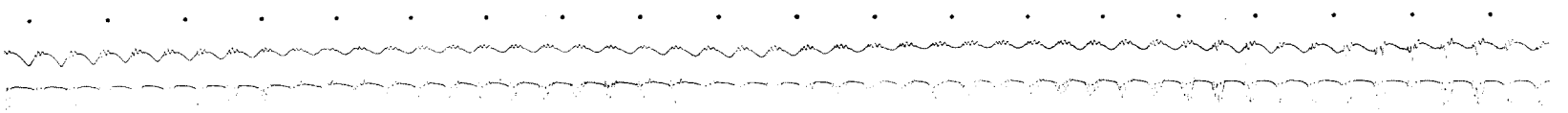

Δz = 0.1 IN. y = 0.12 IN. LOWER TRACE, PEAK

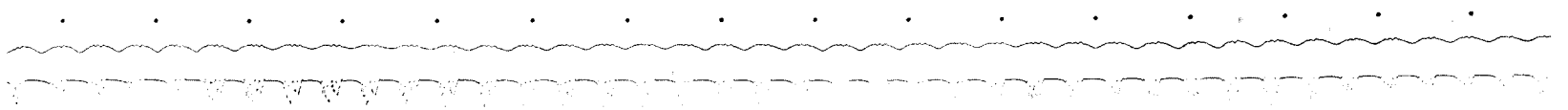

Δz = 0.2 IN. y = 0.12 IN. LOWER TRACE, PEAK

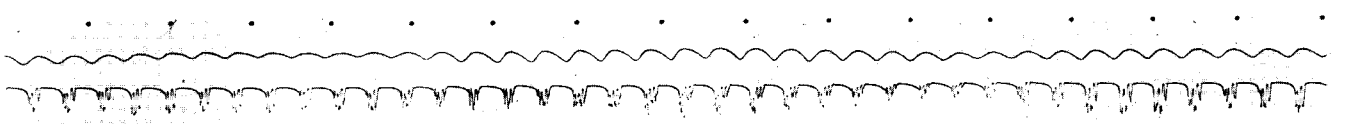

Δz = 0.4 IN. y = 0.12 IN. LOWER TRACE, PEAK

Figure 35. - Oscillograms illustrating extent of breaking pattern in z-direction. y = 0.12 inch; frequency, 145 cps. Time interval between dots, 1/60 second; time progression from right to left; increasing velocity toward timing signal.

$\Delta z = 0$ UPPER TRACE, y = .01 IN. LOWER TRACE, y = .12 IN.

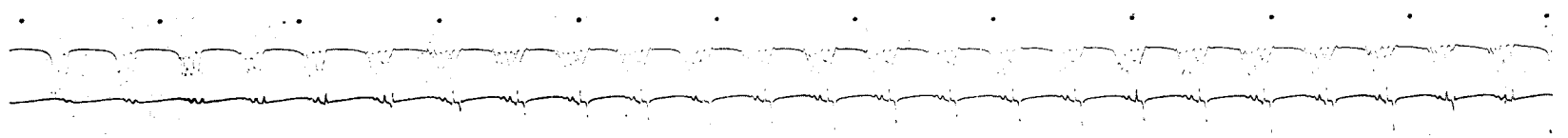

$\Delta z = 0$ UPPER TRACE, y = .12 IN. LOWER TRACE, y = .23 IN.

Figure 36. - Oscillograms illustrating extent of breaking pattern in y-direction. Frequency, 145 cps. Time interval between dots, 1/60 second; time progression from right to left; increasing velocity toward timing signal.

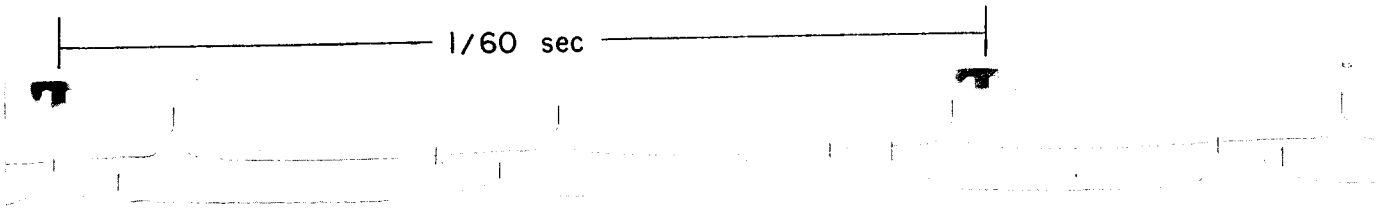


(a) IN REGION OF BREAKDOWN, WIRES SEPARATED 0.52 INCH IN x. DECREASING VELOCITY TOWARD TIMING SIGNAL. $\Delta x$ = 0.52 INCH, y = 0.12 INCH, UPPER TRACE, UPSTREAM WIRE.

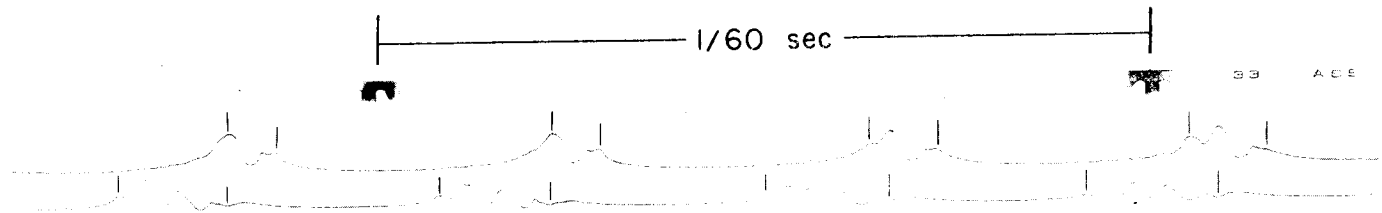


(b) LATER STAGE OF BREAKDOWN THAN (a). IN REGION OF BREAKDOWN, WIRES SEPARATED 0.52 INCH IN x. DECREASING VELOCITY TOWARD TIMING SIGNAL. $\Delta x$ = 0.52 INCH, y = 0.12 INCH, UPPER TRACE, UPSTREAM WIRE.

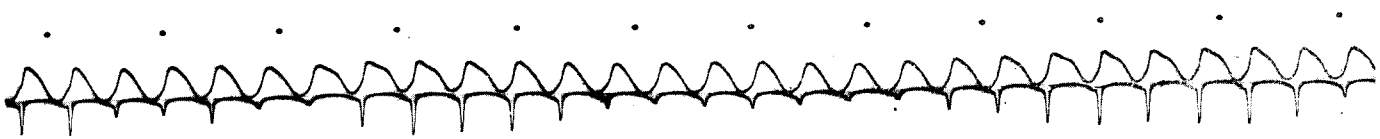

(c) AT INITIAL STAGE OF BREAKDOWN, WIRES SEPARATED 0.115 INCH IN y. INCREASING VELOCITY TOWARD TIMING SIGNAL, TIME INTERVAL BETWEEN DOTS, 1/60 SECOND. $\Delta x$ = 0, $\Delta y$ = 0.115 INCH, UPPER TRACE, y = 0.005 INCH.

Figure 37. - Oscillograms showing simultaneous signals from two hot wires. Time progression from right to left.

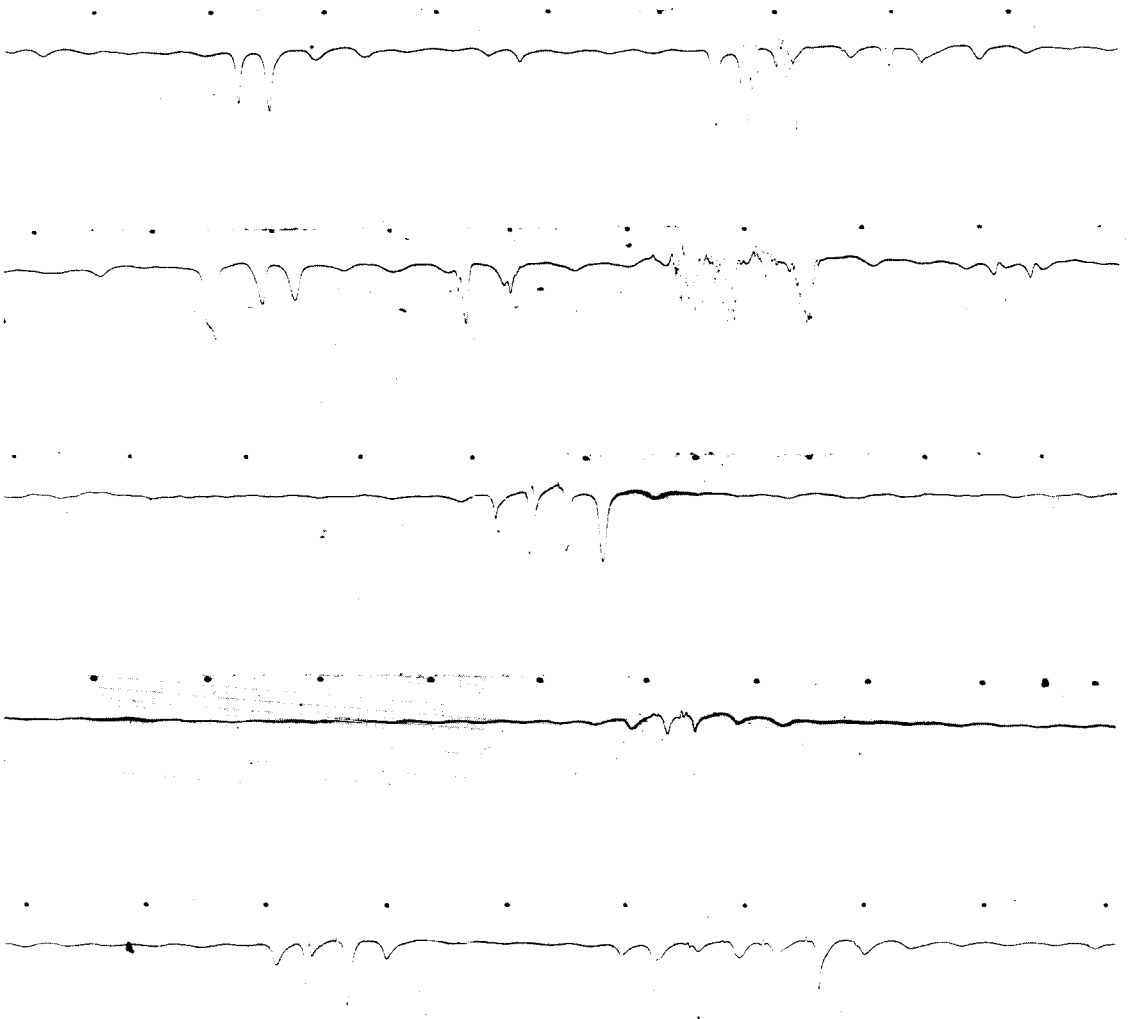


Figure 38. - Oscillograms illustrating occurrence of characteristic breakdown patterns in natural transition.